Flavour Physics and CP-Violation

A. Pich
IFIC, University of València–CSIC, València, Spain

Abstract
An introductory overview of the Standard Model description of flavour is presented. The main emphasis is put on present tests of the quark-mixing matrix structure and the phenomenological determination of its parameters. Special attention is given to the experimental evidence for CP-violation and its important role in our understanding of flavour dynamics.

1 Fermion families

We have learnt experimentally that there are six different quark flavours (u, d, s, c, b, t), three different charged leptons (e, μ, τ) and their corresponding neutrinos (ν_e, ν_μ, ν_τ). We can include all these particles into the $\mathrm{SU}(3)_C \otimes \mathrm{SU}(2)_L \otimes \mathrm{U}(1)_Y$ Standard Model (SM) framework [1–3], by organizing them into three families of quarks and leptons:

$$\begin{bmatrix} \nu_\mathrm{e} & \mathrm{u} \\ \mathrm{e}^- & \mathrm{d}' \end{bmatrix}, \qquad \begin{bmatrix} \nu_\mu & \mathrm{c} \\ \mu^- & \mathrm{s}' \end{bmatrix}, \qquad \begin{bmatrix} \nu_\tau & \mathrm{t} \\ \tau^- & \mathrm{b}' \end{bmatrix}, \tag{1}$$

where (each quark appears in three different colours)

$$\begin{bmatrix} \nu_i & \mathrm{u}_i \\ \ell_i^- & \mathrm{d}_i' \end{bmatrix} \equiv \begin{pmatrix} \nu_i \\ \ell_i^- \end{pmatrix}_L, \quad \begin{pmatrix} \mathrm{u}_i \\ \mathrm{d}_i' \end{pmatrix}_L, \quad \ell_{iR}^-, \quad \mathrm{u}_{iR}, \quad \mathrm{d}_{iR}', \tag{2}$$

plus the corresponding antiparticles. Thus, the left-handed fields are $\mathrm{SU}(2)_L$ doublets, while their right-handed partners transform as $\mathrm{SU}(2)_L$ singlets. The three fermionic families appear to have identical properties (gauge interactions); they differ only by their mass and their flavour quantum number.

The fermionic couplings of the photon and the Z boson are flavour-conserving, i.e. the neutral gauge bosons couple to a fermion and its corresponding antifermion. In contrast, the $\mathrm{W}^\pm$ bosons couple any up-type quark with all down-type quarks because the weak doublet partner of u_i turns out to be a quantum superposition of down-type mass eigenstates: $\mathrm{d}_i' = \sum_j \mathbf{V}_{ij}\, \mathrm{d}_j$. This flavour mixing generates a rich variety of observable phenomena, including CP-violation effects, which can be described in a very successful way within the SM [4].

In spite of its enormous phenomenological success, the SM does not provide any real understanding of flavour. We do not know yet why fermions are replicated in three (and only three) nearly identical copies. Why is the pattern of masses and mixings what it is? Are the masses the only difference among the three families? What is the origin of the SM flavour structure? Which dynamics is responsible for the observed CP-violation? The fermionic flavour is the main source of arbitrary free parameters in the SM: nine fermion masses, three mixing angles and one complex phase, for massless neutrinos. Seven (nine) additional parameters arise with non-zero Dirac (Majorana) neutrino masses: three masses, three mixing angles and one (three) phases. The problem of fermion mass generation is deeply related to the mechanism responsible for the electroweak spontaneous symmetry breaking (SSB). Thus, the origin of these parameters lies in the most obscure part of the SM Lagrangian: the scalar sector. Clearly, the dynamics of flavour appears to be *terra incognita* that deserves a careful investigation.

The following sections contain a short overview of the quark flavour sector and its present phenomenological status. The most relevant experimental tests are briefly described. A more pedagogic introduction to the SM can be found in [4].

2 Flavour structure of the Standard Model

In the SM, flavour-changing transitions occur only in the charged-current sector (Fig. 1):

$$\mathcal{L}_{\rm CC} = -\frac{\rm g}{2\sqrt{2}} \left\{ W_\mu^\dagger \left[\sum_{ij} \bar{\rm u}_i \gamma^\mu (1-\gamma_5) \mathbf{V}_{ij} {\rm d}_j + \sum_\ell \bar\nu_\ell \gamma^\mu (1-\gamma_5) \ell \right] + {\rm h.c.} \right\} . \qquad (3)$$

Fig. 1: Flavour-changing transitions through the charged-current couplings of the $\rm W^\pm$ bosons.

The so-called Cabibbo–Kobayashi–Maskawa (CKM) matrix $\mathbf{V}$ [5, 6] is generated by the same Yukawa couplings giving rise to the quark masses. Before SSB, there is no mixing among the different quarks, i.e. $\mathbf{V} = \mathbf{I}$. In order to understand the origin of the matrix $\mathbf{V}$, let us consider the general case of N_G generations of fermions, and denote ν'_j, ℓ'_j, ${\rm u}'_j$ and ${\rm d}'_j$ the members of the weak family j ($j = 1, \ldots, N_G$), with definite transformation properties under the gauge group. Owing to the fermion replication, a large variety of fermion-scalar couplings are allowed by the gauge symmetry. The most general Yukawa Lagrangian has the form

$$\begin{aligned} \mathcal{L}_Y \;&=\; -\sum_{jk} \left\{ \left(\bar{\rm u}'_j, \bar{\rm d}'_j\right)_L \left[c_{jk}^{(\rm d)} \begin{pmatrix} \phi^{(+)} \\ \phi^{(0)} \end{pmatrix} {\rm d}'_{kR} + c_{jk}^{(\rm u)} \begin{pmatrix} \phi^{(0)*} \\ -\phi^{(-)} \end{pmatrix} {\rm u}'_{kR} \right] \right. \\ &\qquad \left. + \left(\bar\nu'_j, \bar\ell'_j\right)_L c_{jk}^{(\ell)} \begin{pmatrix} \phi^{(+)} \\ \phi^{(0)} \end{pmatrix} \ell'_{kR} \right\} + {\rm h.c.}, \end{aligned} \qquad (4)$$

where $\phi^T(x) \equiv (\phi^{(+)}, \phi^{(0)})$ is the SM scalar doublet and $c_{jk}^{(\rm d)}$, $c_{jk}^{(\rm u)}$ and $c_{jk}^{(\ell)}$ are arbitrary coupling constants. The second term involves the $\mathcal{C}$-conjugate scalar field $\phi^c(x) \equiv {\rm i}\sigma_2 \phi^*(x)$.

In the unitary gauge, $\phi^T(x) \equiv (1/\sqrt{2})(0, v + H)$, where v is the electroweak vacuum expectation value and $H(x)$ the Higgs field. The Yukawa Lagrangian can then be written as

$$\mathcal{L}_Y = -\left(1 + \frac{H}{v}\right) \left\{ \overline{\mathbf{d}}'_L \mathbf{M}'_{\rm d} \mathbf{d}'_R + \overline{\mathbf{u}}'_L \mathbf{M}'_{\rm u} \mathbf{u}'_R + \overline{\boldsymbol{\ell}}'_L \mathbf{M}'_\ell \boldsymbol{\ell}'_R + {\rm h.c.} \right\} . \qquad (5)$$

Here, $\mathbf{d}'$, $\mathbf{u}'$ and $\boldsymbol{\ell}'$ denote vectors in the N_G-dimensional flavour space, with components ${\rm d}'_j$, ${\rm u}'_j$ and ℓ'_j, respectively, and the corresponding mass matrices are given by

$$(\mathbf{M}'_{\rm d})_{ij} \equiv c_{ij}^{(\rm d)} \frac{v}{\sqrt{2}}, \qquad (\mathbf{M}'_{\rm u})_{ij} \equiv c_{ij}^{(\rm u)} \frac{v}{\sqrt{2}}, \qquad (\mathbf{M}'_\ell)_{ij} \equiv c_{ij}^{(\ell)} \frac{v}{\sqrt{2}} . \qquad (6)$$

The diagonalization of these mass matrices determines the mass eigenstates ${\rm d}_j$, ${\rm u}_j$ and ℓ_j, which are linear combinations of the corresponding weak eigenstates ${\rm d}'_j$, ${\rm u}'_j$ and ℓ'_j, respectively.

The matrix $\mathbf{M}'_{\rm d}$ can be decomposed as[1] $\mathbf{M}'_{\rm d} = \mathbf{H}_{\rm d} \mathbf{U}_{\rm d} = \mathbf{S}_{\rm d}^\dagger \mathcal{M}_{\rm d} \mathbf{S}_{\rm d} \mathbf{U}_{\rm d}$, where $\mathbf{H}_{\rm d} \equiv \sqrt{\mathbf{M}'_{\rm d} \mathbf{M}'^\dagger_{\rm d}}$ is a hermitian positive-definite matrix, while $\mathbf{U}_{\rm d}$ is unitary. $\mathbf{H}_{\rm d}$ can be diagonalized by a unitary matrix $\mathbf{S}_{\rm d}$;

[1]The condition $\det \mathbf{M}'_f \neq 0$ ($f = {\rm d, u}, \ell$) guarantees that the decomposition $\mathbf{M}'_f = \mathbf{H}_f \mathbf{U}_f$ is unique: $\mathbf{U}_f \equiv \mathbf{H}_f^{-1} \mathbf{M}'_f$. The matrices $\mathbf{S}_f$ are completely determined (up to phases) only if all diagonal elements of $\mathcal{M}_f$ are different. If there is some degeneracy, the arbitrariness of $\mathbf{S}_f$ reflects the freedom to define the physical fields. If $\det \mathbf{M}'_f = 0$, the matrices $\mathbf{U}_f$ and $\mathbf{S}_f$ are not uniquely determined, unless their unitarity is explicitly imposed.

the resulting matrix $\mathcal{M}_{\rm d}$ is diagonal, hermitian and positive-definite. Similarly, one has $\mathbf{M}'_{\rm u} = \mathbf{H}_{\rm u}\mathbf{U}_{\rm u} = \mathbf{S}_{\rm u}^\dagger \mathcal{M}_{\rm u}\mathbf{S}_{\rm u}\mathbf{U}_{\rm u}$ and $\mathbf{M}'_\ell = \mathbf{H}_\ell\mathbf{U}_\ell = \mathbf{S}_\ell^\dagger\mathcal{M}_\ell\mathbf{S}_\ell\mathbf{U}_\ell$. In terms of the diagonal mass matrices

$$\mathcal{M}_{\rm d} = {\rm diag}(m_{\rm d}, m_{\rm s}, m_{\rm b}, \ldots), \quad \mathcal{M}_{\rm u} = {\rm diag}(m_{\rm u}, m_{\rm c}, m_{\rm t}, \ldots), \quad \mathcal{M}_\ell = {\rm diag}(m_{\rm e}, m_\mu, m_\tau, \ldots), \tag{7}$$

the Yukawa Lagrangian takes the simpler form

$$\mathcal{L}_Y = -\left(1+\frac{H}{v}\right)\left\{\bar{\mathbf{d}}\mathcal{M}_{\rm d}\mathbf{d} + \bar{\mathbf{u}}\mathcal{M}_{\rm u}\mathbf{u} + \bar{\boldsymbol{\ell}}\mathcal{M}_\ell\boldsymbol{\ell}\right\}, \tag{8}$$

where the mass eigenstates are defined by

$$\begin{array}{llll} \mathbf{d}_L \equiv \mathbf{S}_{\rm d}\,\mathbf{d}'_L\,, & \mathbf{u}_L \equiv \mathbf{S}_{\rm u}\,\mathbf{u}'_L\,, & \boldsymbol{\ell}_L \equiv \mathbf{S}_\ell\,\boldsymbol{\ell}'_L\,, & \\ \mathbf{d}_R \equiv \mathbf{S}_{\rm d}\mathbf{U}_{\rm d}\,\mathbf{d}'_R\,, & \mathbf{u}_R \equiv \mathbf{S}_{\rm u}\mathbf{U}_{\rm u}\,\mathbf{u}'_R\,, & \boldsymbol{\ell}_R \equiv \mathbf{S}_\ell\mathbf{U}_\ell\,\boldsymbol{\ell}'_R\,. & (9) \end{array}$$

Note that the Higgs couplings are proportional to the corresponding fermion masses.

Since $\bar{\mathbf{f}}'_L\,\mathbf{f}'_L = \bar{\mathbf{f}}_L\,\mathbf{f}_L$ and $\bar{\mathbf{f}}'_R\,\mathbf{f}'_R = \bar{\mathbf{f}}_R\,\mathbf{f}_R$ ($f = {\rm d}, {\rm u}, \ell$), the form of the neutral-current part of the $SU(3)_C \otimes SU(2)_L \otimes U(1)_Y$ Lagrangian does not change when expressed in terms of mass eigenstates. Therefore, there are no flavour-changing neutral currents in the SM (Glashow–Iliopoulos–Maiani (GIM) mechanism [7]). This is a consequence of treating all equal-charge fermions on the same footing. However, $\bar{\mathbf{u}}'_L\,\mathbf{d}'_L = \bar{\mathbf{u}}_L\,\mathbf{S}_{\rm u}\,\mathbf{S}_{\rm d}^\dagger\,\mathbf{d}_L \equiv \bar{\mathbf{u}}_L\mathbf{V}\,\mathbf{d}_L$. In general, $\mathbf{S}_{\rm u} \neq \mathbf{S}_{\rm d}$; thus, if one writes the weak eigenstates in terms of mass eigenstates, an $N_G \times N_G$ unitary mixing matrix $\mathbf{V}$ appears in the quark charged-current sector as indicated in Eq. (3).

If neutrinos are assumed to be massless, we can always redefine the neutrino flavours, in such a way as to eliminate the mixing in the lepton sector: $\bar{\boldsymbol{\nu}}'_L\,\boldsymbol{\ell}'_L = \bar{\boldsymbol{\nu}}'_L\,\mathbf{S}_\ell^\dagger\,\boldsymbol{\ell}_L \equiv \bar{\boldsymbol{\nu}}_L\,\boldsymbol{\ell}_L$. Thus, we have lepton-flavour conservation in the minimal SM without right-handed neutrinos. If sterile ν_R fields are included in the model, one has an additional Yukawa term in Eq. (4), giving rise to a neutrino mass matrix $(\mathbf{M}'_\nu)_{ij} \equiv c_{ij}^{(\nu)}\,v/\sqrt{2}$. Thus, the model can accommodate non-zero neutrino masses and lepton-flavour violation through a lepton-mixing matrix $\mathbf{V}_L$ analogous to the one present in the quark sector. Note, however, that the total lepton number $L \equiv L_{\rm e} + L_\mu + L_\tau$ is still conserved. We know experimentally that neutrino masses are tiny and, as shown in Table 1, there are strong bounds on lepton-flavour-violating decays. However, we do have clear evidence of neutrino oscillation phenomena. Moreover, since right-handed neutrinos are singlets under $SU(3)_C \otimes SU(2)_L \otimes U(1)_Y$, the SM gauge symmetry group allows for a right-handed Majorana neutrino mass term, violating lepton number by two units. Non-zero neutrino masses clearly imply interesting new phenomena [4].

The fermion masses and the quark-mixing matrix $\mathbf{V}$ are all determined by the Yukawa couplings in Eq. (4). However, the coefficients $c_{ij}^{(f)}$ are not known; therefore, we have a bunch of arbitrary parameters. A general $N_G \times N_G$ unitary matrix is characterized by N_G^2 real parameters: $N_G(N_G-1)/2$ moduli

Table 1: Experimental upper limits (90% confidence level (CL)) on lepton-flavour-violating decays [8–12].

$Br(\mu^- \to X^-) \times 10^{12}$									
$e^-\gamma$	2.4	$e^-2\gamma$	72	$e^-e^-e^+$	1.0				
$Br(\tau^- \to X^-) \times 10^{8}$									
$\mu^-\gamma$	4.4	$e^-\gamma$	3.3	$\mu^-\mu^+\mu^-$	2.1	$\mu^-\pi^+\pi^-$	3.3	$\mu^-K^+K^-$	6.8
$\mu^-\pi^0$	11	$e^-\pi^0$	8.0	$e^-\mu^+\mu^-$	2.7	$e^-\pi^+\pi^-$	4.4	$e^-K^+K^-$	5.4
μ^-K_S	2.3	e^-K_S	2.6	$\mu^-e^+e^-$	1.8	$\mu^+\pi^-\pi^-$	3.7	$e^-K^\pm\pi^\mp$	5.8
$\mu^-\rho^0$	2.6	$e^-\phi$	3.1	$e^-e^+e^-$	2.7	$e^+\pi^-\pi^-$	8.8	$e^+K^-K^-$	6.0
$\mu^-\eta$	6.5	$e^-\eta$	9.2	$\mu^-\mu^-e^+$	1.7	$\mu^-\omega$	8.9	$e^+K^-\pi^-$	6.7
μ^-K^{*0}	5.9	e^-K^{*0}	5.9	$e^-e^-\mu^+$	1.5	$\Lambda\pi^-$	7.2	$\mu^+K^-\pi^-$	9.4

and $N_G(N_G+1)/2$ phases. In the case of $\mathbf{V}$, many of these parameters are irrelevant because we can always choose arbitrary quark phases. Under the phase redefinitions $\mathrm{u}_i \to \mathrm{e}^{\mathrm{i}\phi_i}\,\mathrm{u}_i$ and $\mathrm{d}_j \to \mathrm{e}^{\mathrm{i}\theta_j}\,\mathrm{d}_j$, the mixing matrix changes as $\mathbf{V}_{ij} \to \mathbf{V}_{ij}\,\mathrm{e}^{\mathrm{i}(\theta_j-\phi_i)}$; thus, $2N_G-1$ phases are unobservable. The number of physical free parameters in the quark-mixing matrix then gets reduced to $(N_G-1)^2$: $N_G(N_G-1)/2$ moduli and $(N_G-1)(N_G-2)/2$ phases.

In the simpler case of two generations, $\mathbf{V}$ is determined by a single parameter. One then recovers the Cabibbo rotation matrix [5]

$$\mathbf{V} = \begin{pmatrix} \cos\theta_C & \sin\theta_C \\ -\sin\theta_C & \cos\theta_C \end{pmatrix} . \tag{10}$$

With $N_G = 3$, the CKM matrix is described by three angles and one phase. Different (but equivalent) representations can be found in the literature. The Particle Data Group (PDG) [13] advocates the use of the following one as the 'standard' CKM parametrization:

$$\mathbf{V} = \begin{bmatrix} c_{12}\,c_{13} & s_{12}\,c_{13} & s_{13}\,\mathrm{e}^{-\mathrm{i}\delta_{13}} \\ -s_{12}\,c_{23} - c_{12}\,s_{23}\,s_{13}\,\mathrm{e}^{\mathrm{i}\delta_{13}} & c_{12}\,c_{23} - s_{12}\,s_{23}\,s_{13}\,\mathrm{e}^{\mathrm{i}\delta_{13}} & s_{23}\,c_{13} \\ s_{12}\,s_{23} - c_{12}\,c_{23}\,s_{13}\,\mathrm{e}^{\mathrm{i}\delta_{13}} & -c_{12}\,s_{23} - s_{12}\,c_{23}\,s_{13}\,\mathrm{e}^{\mathrm{i}\delta_{13}} & c_{23}\,c_{13} \end{bmatrix} . \tag{11}$$

Here $c_{ij} \equiv \cos\theta_{ij}$ and $s_{ij} \equiv \sin\theta_{ij}$, with i and j being generation labels ($i,j = 1,2,3$). The real angles θ_{12}, θ_{23} and θ_{13} can all be made to lie in the first quadrant, by an appropriate redefinition of quark field phases; then $c_{ij} \geq 0$, $s_{ij} \geq 0$ and $0 \leq \delta_{13} \leq 2\pi$. Note that δ_{13} is the only complex phase in the SM Lagrangian. Therefore, it is the only possible source of CP-violation phenomena. In fact, it was for this reason that the third generation was assumed to exist [6], before the discovery of the b and the τ. With two generations, the SM could not explain the observed CP-violation in the K system.

3 Lepton decays

The simplest flavour-changing process is the leptonic decay of the muon, which proceeds through the W-exchange diagram shown in Fig. 2. The momentum transfer carried by the intermediate W is very small compared to M_{W}. Therefore, the vector-boson propagator reduces to a contact interaction,

$$\frac{-g_{\mu\nu} + q_\mu q_\nu/M_{\mathrm{W}}^2}{q^2 - M_{\mathrm{W}}^2} \;\stackrel{q^2 \ll M_{\mathrm{W}}^2}{\longrightarrow}\; \frac{g_{\mu\nu}}{M_{\mathrm{W}}^2} . \tag{12}$$

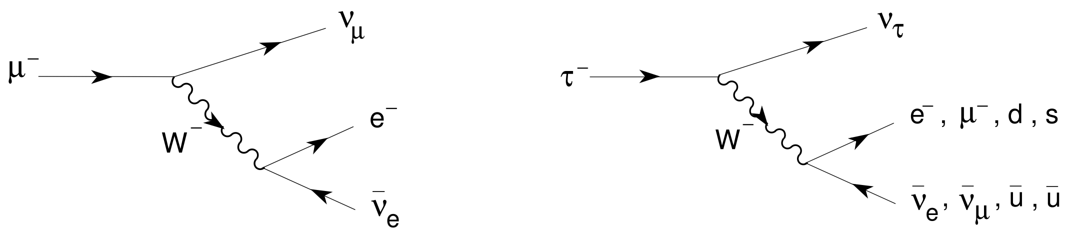

Fig. 2: Tree-level Feynman diagrams for $\mu^- \to \mathrm{e}^-\bar{\nu}_{\mathrm{e}}\nu_\mu$ and $\tau^- \to \nu_\tau \mathrm{X}^-$ ($\mathrm{X}^- = \mathrm{e}^-\bar{\nu}_{\mathrm{e}}, \mu^-\bar{\nu}_\mu, \mathrm{d}\bar{\mathrm{u}}, \mathrm{s}\bar{\mathrm{u}}$).

The decay can then be described through an effective local four-fermion Hamiltonian,

$$\mathcal{H}_{\mathrm{eff}} = \frac{G_F}{\sqrt{2}}\,\left[\bar{\mathrm{e}}\gamma^\alpha(1-\gamma_5)\nu_{\mathrm{e}}\right]\,\left[\bar{\nu}_\mu\gamma_\alpha(1-\gamma_5)\mu\right] , \tag{13}$$

where

$$\frac{G_F}{\sqrt{2}} = \frac{g^2}{8M_{\mathrm{W}}^2} = \frac{1}{2v^2} \tag{14}$$

is called the Fermi coupling constant. G_F is fixed by the total decay width,

$$\frac{1}{\tau_\mu} = \Gamma[\mu^- \to \mathrm{e}^- \bar{\nu}_\mathrm{e} \nu_\mu(\gamma)] = \frac{G_F^2 m_\mu^5}{192\pi^3} (1+\delta_{\mathrm{RC}}) \, f(m_\mathrm{e}^2/m_\mu^2), \tag{15}$$

where $f(x) = 1 - 8x + 8x^3 - x^4 - 12x^2 \ln x$, and

$$1 + \delta_{\mathrm{RC}} = \left[1 + \frac{\alpha}{2\pi}\left(\frac{25}{4} - \pi^2\right)\right] \left[1 + \frac{3}{5}\frac{m_\mu^2}{M_\mathrm{W}^2} - 2\frac{m_\mathrm{e}^2}{M_\mathrm{W}^2}\right] + \cdots \tag{16}$$

contains the radiative higher-order corrections, which are known to $\mathcal{O}(\alpha^2)$ [14–16]. The measured lifetime [17], $\tau_\mu = (2.196\,980\,3 \pm 0.000\,002\,2) \times 10^{-6}$ s, implies the value

$$G_F = (1.166\,378\,8 \pm 0.000\,000\,7) \times 10^{-5}\ \mathrm{GeV}^{-2} \approx \frac{1}{(293\ \mathrm{GeV})^2}\,. \tag{17}$$

The decays of the τ lepton proceed through the same W-exchange mechanism. The only difference is that several final states are kinematically allowed: $\tau^- \to \nu_\tau \mathrm{e}^- \bar{\nu}_\mathrm{e}$, $\tau^- \to \nu_\tau \mu^- \bar{\nu}_\mu$, $\tau^- \to \nu_\tau \mathrm{d}\bar{\mathrm{u}}$ and $\tau^- \to \nu_\tau \mathrm{s}\bar{\mathrm{u}}$. Owing to the universality of the W couplings, all these decay modes have equal amplitudes (if final fermion masses and quantum chromodynamic (QCD) interactions are neglected), except for an additional $N_C|\mathbf{V}_{\mathrm{u}i}|^2$ factor ($i = \mathrm{d,s}$) in the semileptonic channels, where $N_C = 3$ is the number of quark colours. Making trivial kinematic changes in Eq. (15), one easily gets the lowest-order prediction for the total τ decay width:

$$\frac{1}{\tau_\tau} \equiv \Gamma(\tau) \approx \Gamma(\mu)\left(\frac{m_\tau}{m_\mu}\right)^5 \left\{2 + N_C\left(|\mathbf{V}_{\mathrm{ud}}|^2 + |\mathbf{V}_{\mathrm{us}}|^2\right)\right\} \approx \frac{5}{\tau_\mu}\left(\frac{m_\tau}{m_\mu}\right)^5, \tag{18}$$

where we have used the CKM unitarity relation $|\mathbf{V}_{\mathrm{ud}}|^2 + |\mathbf{V}_{\mathrm{us}}|^2 = 1 - |\mathbf{V}_{\mathrm{ub}}|^2 \approx 1$ (we will see later that this is an excellent approximation). From the measured muon lifetime, one then has $\tau_\tau \approx 3.3 \times 10^{-13}$ s, to be compared with the experimental value [13] $\tau_\tau^{\mathrm{exp}} = (2.906 \pm 0.010) \times 10^{-13}$ s. The numerical difference is due to the effect of QCD corrections, which enhance the hadronic τ decay width by about 20%. The size of these corrections has been accurately predicted in terms of the strong coupling [18], allowing us to extract from τ decays one of the most precise determinations of α_s [19].

In the SM, all lepton doublets have identical couplings to the W boson. Comparing the measured decay widths of leptonic or semileptonic decays that only differ in the lepton flavour, one can test experimentally that the W interaction is indeed the same, i.e. that $g_\mathrm{e} = g_\mu = g_\tau \equiv g$. As shown in Table 2, the present data verify the universality of the leptonic charged-current couplings to the 0.2% level.

Table 2: Experimental determinations of the ratios $g_\ell/g_{\ell'}$ [13, 20–22].

	$\Gamma_{\tau\to\mu}/\Gamma_{\tau\to\mathrm{e}}$	$\Gamma_{\pi\to\mu}/\Gamma_{\pi\to\mathrm{e}}$	$\Gamma_{\mathrm{K}\to\mu}/\Gamma_{\mathrm{K}\to\mathrm{e}}$	$\Gamma_{\mathrm{K}\to\pi\mu}/\Gamma_{\mathrm{K}\to\pi\mathrm{e}}$	$\Gamma_{\mathrm{W}\to\mu}/\Gamma_{\mathrm{W}\to\mathrm{e}}$
$\lvert g_\mu/g_\mathrm{e}\rvert$	1.0018 (14)	1.0021 (16)	0.998 (2)	1.001 (2)	0.991 (9)
	$\Gamma_{\tau\to\mathrm{e}}/\Gamma_{\mu\to\mathrm{e}}$	$\Gamma_{\tau\to\pi}/\Gamma_{\pi\to\mu}$	$\Gamma_{\tau\to\mathrm{K}}/\Gamma_{\mathrm{K}\to\mu}$	$\Gamma_{\mathrm{W}\to\tau}/\Gamma_{\mathrm{W}\to\mu}$	
$\lvert g_\tau/g_\mu\rvert$	1.0007 (22)	0.992 (4)	0.982 (8)	1.032 (12)	
	$\Gamma_{\tau\to\mu}/\Gamma_{\mu\to\mathrm{e}}$	$\Gamma_{\mathrm{W}\to\tau}/\Gamma_{\mathrm{W}\to\mathrm{e}}$			
$\lvert g_\tau/g_\mathrm{e}\rvert$	1.0016 (21)	1.023 (11)			

4 Quark mixing

In order to measure the CKM matrix elements, one needs to study hadronic weak decays of the type $\mathrm{H} \to \mathrm{H}'\ell^-\bar{\nu}_\ell$ or $\mathrm{H} \to \mathrm{H}'\ell^+\nu_\ell$, which are associated with the corresponding quark transitions $\mathrm{d}_j \to \mathrm{u}_i\, \ell^-\bar{\nu}_\ell$ and $\mathrm{u}_i \to \mathrm{d}_j\, \ell^+\nu_\ell$ (Fig. 3). Since quarks are confined within hadrons, the decay amplitude

$$T[\mathrm{H} \to \mathrm{H}'\ell^-\bar{\nu}_\ell] \;\approx\; \frac{G_F}{\sqrt{2}}\, \mathbf{V}_{ij}\;\langle \mathrm{H}'|\, \bar{\mathrm{u}}_i\, \gamma^\mu(1-\gamma_5)\, \mathrm{d}_j\, |\mathrm{H}\rangle\;\; [\bar{\ell}\gamma_\mu(1-\gamma_5)\nu_\ell] \tag{19}$$

always involves a hadronic matrix element of the weak left current. The evaluation of this matrix element is a non-perturbative QCD problem, which introduces unavoidable theoretical uncertainties.

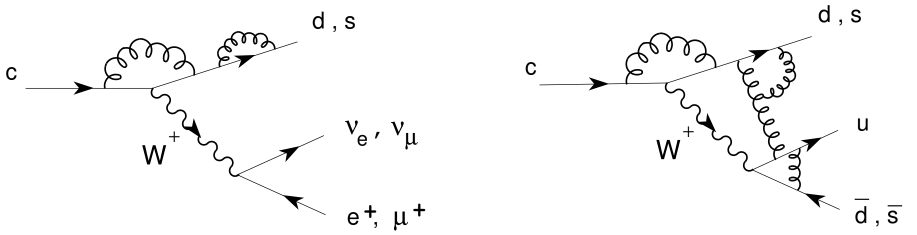

Fig. 3: (left) Matrix elements $\mathbf{V}_{ij}$ are measured in semileptonic decays, where a single quark current is present. (right) Hadronic decays involve two different quark currents and are more affected by QCD effects (gluons can couple everywhere).

One usually looks for a semileptonic transition where the matrix element can be fixed at some kinematic point by a symmetry principle. This has the virtue of reducing the theoretical uncertainties to the level of symmetry-breaking corrections and kinematic extrapolations. The standard example is a $0^- \to 0^-$ decay such as $\mathrm{K} \to \pi\ell\nu_\ell$, $\mathrm{D} \to \mathrm{K}\ell\nu_\ell$ or $\mathrm{B} \to \mathrm{D}\ell\nu_\ell$. Only the vector current can contribute in this case:

$$\langle P'(k')|\, \bar{\mathrm{u}}_i\, \gamma^\mu\, \mathrm{d}_j\, |P(k)\rangle \;=\; C_{PP'}\, \left\{ (k+k')^\mu\, f_+(t) \,+\, (k-k')^\mu\, f_-(t) \right\} . \tag{20}$$

Here, $C_{PP'}$ is a Clebsch–Gordan factor and $t = (k-k')^2 \equiv q^2$. The unknown strong dynamics is fully contained in the form factors $f_\pm(t)$. In the limit of equal quark masses, $m_{\mathrm{u}_i} = m_{\mathrm{d}_j}$, the divergence of the vector current is zero; thus $q_\mu\, [\bar{\mathrm{u}}_i\gamma^\mu \mathrm{d}_j] = 0$, which implies $f_-(t) = 0$ and, moreover, $f_+(0) = 1$ to all orders in the strong coupling because the associated flavour charge is a conserved quantity.[2] Therefore, one only needs to estimate the corrections induced by the quark mass differences.

Since $q^\mu[\bar{\ell}\gamma_\mu(1-\gamma_5)\nu_\ell] \sim m_\ell$, the contribution of $f_-(t)$ is kinematically suppressed in the electron and muon modes. The decay width can then be written as

$$\Gamma(P \to P'l\nu) \;=\; \frac{G_F^2 M_P^5}{192\pi^3}\, |\mathbf{V}_{ij}|^2\, C_{PP'}^2\, |f_+(0)|^2\, \mathcal{I}(1+\delta_{\mathrm{RC}}), \tag{21}$$

where δ_{RC} is an electroweak radiative correction factor and $\mathcal{I}$ denotes a phase-space integral, which in the $m_\ell = 0$ limit takes the form

$$\mathcal{I} \;\approx\; \int_0^{(M_P - M_{P'})^2} \frac{\mathrm{d}t}{M_P^8}\, \lambda^{3/2}(t, M_P^2, M_{P'}^2)\, \left|\frac{f_+(t)}{f_+(0)}\right|^2 . \tag{22}$$

The usual procedure to determine $|\mathbf{V}_{ij}|$ involves three steps:

1. Measure the shape of the t distribution. This fixes $|f_+(t)/f_+(0)|$ and therefore determines $\mathcal{I}$.

[2] This is completely analogous to the electromagnetic charge conservation in quantum electrodynamics (QED). The conservation of the electromagnetic current implies that the proton electromagnetic form factor does not get any QED or QCD correction at $q^2 = 0$ and, therefore, $Q(p) = 2Q(\mathrm{u}) + Q(\mathrm{d}) = |Q(\mathrm{e})|$. A detailed proof can be found in [23].

2. Measure the total decay width Γ. Since G_F is already known from μ decay, one then gets an experimental value for the product $|f_+(0)\,\mathbf{V}_{ij}|$.
3. Get a theoretical prediction for $f_+(0)$.

It is important to realize that theoretical input is always needed. Thus, the accuracy of the $|\mathbf{V}_{ij}|$ determination is limited by our ability to calculate the relevant hadronic parameters.

4.1 Determination of $|\mathbf{V_{ud}}|$ and $|\mathbf{V_{us}}|$

The conservation of the vector QCD currents in the massless quark limit allows for precise determinations of the light-quark mixings. The most accurate measurement of $\mathbf{V}_{\rm ud}$ is done with super-allowed nuclear beta decays of the Fermi type ($0^+ \to 0^+$), where the nuclear matrix element $\langle N'|\bar{\rm u}\gamma^\mu {\rm d}|N\rangle$ can be fixed by vector-current conservation. The CKM factor is obtained through the relation [24, 25],

$$|\mathbf{V}_{\rm ud}|^2 \; = \; \frac{\pi^3 \ln 2}{ft\, G_F^2 m_{\rm e}^5\, (1+\delta_{\rm RC})} \; = \; \frac{(2984.48 \pm 0.05)\ {\rm s}}{ft\, (1+\delta_{\rm RC})}\,, \tag{23}$$

where ft denotes the product of a phase-space statistical decay-rate factor and the measured half-life. In order to obtain $|\mathbf{V}_{\rm ud}|$, one needs to perform a careful analysis of radiative corrections, including electroweak contributions, nuclear-structure corrections and isospin-violating nuclear effects. These nuclear-dependent corrections are quite large, $\delta_{\rm RC} \sim$ 3–4%, and have a crucial role in bringing the results from different nuclei into good agreement. The weighted average of the 20 most precise determinations yields [26]

$$|\mathbf{V}_{\rm ud}| \; = \; 0.974\,25 \pm 0.000\,22. \tag{24}$$

A nuclear-physics-independent determination can be obtained from neutron decay, ${\rm n} \to {\rm p\, e^-} \bar\nu_{\rm e}$. The axial current also contributes in this case; therefore, one needs to use the experimental value of the axial-current matrix element at $q^2 = 0$, $\langle {\rm p}\,|\,\bar{\rm u}\gamma^\mu\gamma_5 {\rm d}\,|\,{\rm n}\rangle = G_A\, \bar{\rm p}\gamma^\mu {\rm n}$. The present world averages, $g_A \equiv G_A/G_V = -1.2701 \pm 0.0025$ and $\tau_{\rm n} = (881.5 \pm 1.5)$ s, imply [13, 24, 25]

$$|\mathbf{V}_{\rm ud}| \; = \; \left\{ \frac{(4908.7 \pm 1.9)\ {\rm s}}{\tau_{\rm n}\, (1+3g_A^2)} \right\}^{1/2} \; = \; 0.9765 \pm 0.0018\,, \tag{25}$$

which is larger but less precise than the value in (24).

The experimental determination of the neutron lifetime is controversial. The most precise measurement, $\tau_{\rm n} = (878.5 \pm 0.8)$ s [27], disagrees by 6σ from the 2010 PDG average $\tau_{\rm n} = (885.7 \pm 0.8)$ s [13], from which it was excluded. Since a more recent experiment [28] finds a mean life closer to the value given in [27], both results have been included in the 2011 PDG average, enlarging the error with a scale factor of 2.7 to account for the discrepancies. Including only the three most recent measurements [27–29] leads to $\tau_{\rm n} = (879.1 \pm 1.2)$ s; this implies $|\mathbf{V}_{\rm ud}| = 0.9779 \pm 0.0017$, which is 2.1σ larger than the value in (24). Small inconsistencies are also present in the g_A measurements, with the most recent experiments [30] favouring slightly larger values of $|g_A|$. Better measurements of g_A and $\tau_{\rm n}$ are needed.

The pion beta decay $\pi^+ \to \pi^0 {\rm e}^+ \nu_{\rm e}$ offers a cleaner way to measure $|\mathbf{V}_{\rm ud}|$. It is a pure vector transition, with very small theoretical uncertainties. At $q^2 = 0$, the hadronic matrix element does not receive isospin-breaking contributions of first order in $m_{\rm d} - m_{\rm u}$, i.e. $f_+(0) = 1 + \mathcal{O}[(m_{\rm d} - m_{\rm u})^2]$ [31]. The small available phase space makes it possible to control the form factor theoretically with high accuracy over the entire kinematic domain [32]; unfortunately, it also implies a very suppressed branching fraction. From the present experimental value [33], ${\rm Br}(\pi^+ \to \pi^0 {\rm e}^+ \nu_{\rm e}) = (1.040 \pm 0.006) \times 10^{-8}$, one gets $|\mathbf{V}_{\rm ud}| = 0.9741 \pm 0.0002_{\rm th} \pm 0.0026_{\rm exp}$ [34]. A 10-fold improvement of the experimental accuracy would be needed to get a determination competitive with (24).

The classic determination of $|\mathbf{V}_{\rm us}|$ takes advantage of the theoretically well-understood $K_{\ell 3}$ decays. The most recent high-statistics experiments have resulted in significant shifts in the branching fractions and improved precision for all of the experimental inputs [13]. Supplemented with theoretical calculations of electromagnetic and isospin corrections [35, 36], they allow us to extract the product $|\mathbf{V}_{\rm us}\, f_+(0)| = 0.2163 \pm 0.0005$ [22], with $f_+(0) = 1 + \mathcal{O}[(m_{\rm s} - m_{\rm u})^2]$ the vector form factor of the $\mathrm{K}^0 \to \pi^- \ell^+ \nu_\ell$ decay [31, 37]. The exact value of $f_+(0)$ has been thoroughly investigated since the first precise estimate by Leutwyler and Roos [38], $f_+(0) = 0.961 \pm 0.008$. While analytical calculations based on chiral perturbation theory obtain higher values [39, 40], as a consequence of including the large and positive (~ 0.01) two-loop chiral corrections [41], the lattice results [42] tend to agree with the Leutwyler–Roos estimate. Taking as reference value the most recent and precise lattice result [43], $f_+(0) = 0.960 \pm 0.006$, one obtains [44]

$$|\mathbf{V}_{\rm us}| \, = \, 0.2255 \pm 0.0005_{\rm exp} \pm 0.0012_{\rm th} \, . \tag{26}$$

Information on $\mathbf{V}_{\rm us}$ can also be obtained [22, 45] from the ratio of radiative inclusive decay rates $\Gamma[\mathrm{K} \to \mu\nu(\gamma)]/\Gamma[\pi \to \mu\nu(\gamma)]$. With a careful treatment of electromagnetic and isospin-violating corrections, one extracts $|\mathbf{V}_{\rm us}/\mathbf{V}_{\rm ud}|\,|F_{\rm K}/F_\pi| = 0.2763 \pm 0.0005$ [46]. Taking for the ratio of meson decay constants the lattice average $F_{\rm K}/F_\pi = 1.193 \pm 0.006$ [42], one gets [46]

$$\frac{|\mathbf{V}_{\rm us}|}{|\mathbf{V}_{\rm ud}|} \, = \, 0.2316 \pm 0.0012 \, . \tag{27}$$

With the value of $|\mathbf{V}_{\rm ud}|$ in Eq. (24), this implies $|\mathbf{V}_{\rm us}| = 0.2256 \pm 0.0012$.

Hyperon decays are also sensitive to $\mathbf{V}_{\rm us}$ [47]. Unfortunately, in weak baryon decays the theoretical control on SU(3)-breaking corrections is not as good as for the meson case. A conservative estimate of these effects leads to the result $|\mathbf{V}_{\rm us}| = 0.226 \pm 0.005$ [48].

The accuracy of all previous determinations is limited by theoretical uncertainties. The separate measurement of the inclusive $|\Delta S| = 0$ and $|\Delta S| = 1$ tau decay widths provides a very clean observable to measure $|\mathbf{V}_{\rm us}|$ directly [49, 50], because SU(3)-breaking corrections are suppressed by two powers of the τ mass. The present τ decay data imply $|\mathbf{V}_{\rm us}| = 0.2166 \pm 0.0019_{\rm exp} \pm 0.0005_{\rm th}$ [50], the error being dominated by the experimental uncertainties. The central value has been shifted down by the inclusion of the most recent BABAR and BELLE measurements, which find branching ratios smaller than the previous world averages [13]. More precise data are needed to clarify this worrisome effect. If the strangeness-changing τ decay width is measured with a 1% precision, the resulting $\mathbf{V}_{\rm us}$ uncertainty will get reduced to around 0.6%, i.e. ± 0.0013.

4.2 Determination of $|\mathbf{V}_{\rm cb}|$ and $|\mathbf{V}_{\rm ub}|$

In the limit of very heavy quark masses, QCD has additional flavour and spin symmetries [51–54], which can be used to make rather precise determinations of $|\mathbf{V}_{\rm cb}|$, either from exclusive decays [55, 56] or from the inclusive analysis of $\mathrm{b} \to \mathrm{c}\ell\bar{\nu}_\ell$ transitions.

When $m_{\rm b} \gg \Lambda_{\rm QCD}$, all form factors characterizing the decays $\mathrm{B} \to \mathrm{D}\ell\bar{\nu}_\ell$ and $\mathrm{B} \to \mathrm{D}^*\ell\bar{\nu}_\ell$ reduce to a single function [51], which depends on the product of the four-velocities of the two mesons, $w \equiv v_{\rm B} \cdot v_{\mathrm{D}^{(*)}} = (M_{\rm B}^2 + M_{\mathrm{D}^{(*)}}^2 - q^2)/(2 M_{\rm B} M_{\mathrm{D}^{(*)}})$. Heavy-quark symmetry determines the normalization of the rate at $w = 1$, the maximum momentum transfer to the leptons, because the corresponding vector current is conserved in the limit of equal B and $\mathrm{D}^{(*)}$ velocities. The $\mathrm{B} \to \mathrm{D}^*$ mode has the additional advantage that corrections to the infinite-mass limit are of second order in $1/m_{\rm b} - 1/m_{\rm c}$ at zero recoil ($w = 1$) [56]. The exclusive determination of $|\mathbf{V}_{\rm cb}|$ is obtained from an extrapolation of the measured spectrum to $w = 1$. From $\mathrm{B} \to \mathrm{D}^*\ell\bar{\nu}_\ell$ data one gets $|\mathbf{V}_{\rm cb}|\,\mathcal{F}(1) = (36.04 \pm 0.52) \times 10^{-3}$, while the measured $\mathrm{B} \to \mathrm{D}\ell\bar{\nu}_\ell$ distribution results in $|\mathbf{V}_{\rm cb}|\,\mathcal{G}(1) = (42.3 \pm 0.7 \pm 1.3) \times 10^{-3}$ [57]. Lattice simulations are used to estimate the deviations from unity of the two form factors at $w = 1$; the most recent results are $\mathcal{F}(1) = 0.908 \pm 0.017$ [58] and $\mathcal{G}(1) = 1.074 \pm 0.018 \pm 0.016$ [59]. A smaller value $\mathcal{F}(1) = 0.86 \pm 0.03$ is obtained from zero-recoil sum rules [60]. Adopting the lattice estimates, one gets

$$|\mathbf{V}_{\rm cb}| \,=\, \left\{ \begin{array}{ll} (39.7 \pm 0.9) \times 10^{-3} & \quad ({\rm B} \to {\rm D}^* \ell \bar{\nu}_\ell) \\ (39.4 \pm 1.6) \times 10^{-3} & \quad ({\rm B} \to {\rm D} \ell \bar{\nu}_\ell) \end{array} \right. \;=\; (39.6 \pm 0.8) \times 10^{-3} . \qquad (28)$$

The inclusive determination uses the operator product expansion [61, 62] to express the total $\mathrm{b} \to \mathrm{c}\ell\bar{\nu}_\ell$ rate and moments of the differential energy and invariant-mass spectra in a double expansion in powers of α_s and $1/m_{\rm b}$ [63–67], which includes terms of $O(1/m_{\rm b}^3)$ and has recently been upgraded to a complete $O(\alpha_s^2)$ calculation [68]. The non-perturbative matrix elements of the corresponding local operators are obtained from a global fit to experimental moments of inclusive $\mathrm{B} \to \mathrm{X_c}\, \ell\, \bar{\nu}_\ell$ (lepton energy and hadronic invariant mass) and $\mathrm{B} \to \mathrm{X_s}\gamma$ (photon energy spectrum) observables. The combination of 66 different measurements results in [57]

$$|\mathbf{V}_{\rm cb}| \,=\, (41.85 \pm 0.73) \times 10^{-3} \, . \qquad (29)$$

At present there is a 2.1σ discrepancy between the exclusive and inclusive determinations. Following the PDG prescription [13], we average both values by scaling the error by $\sqrt{\chi^2/\mathrm{dof}} = 2.1$ (where dof denotes the number of degrees of freedom):

$$|\mathbf{V}_{\rm cb}| \,=\, (40.8 \pm 1.1) \times 10^{-3} \, . \qquad (30)$$

A similar disagreement is observed for the analogous $|\mathbf{V}_{\rm ub}|$ determinations. The presence of a light quark makes it more difficult to control the theoretical uncertainties. Exclusive $\mathrm{B} \to \pi\ell\nu_\ell$ decays involve a non-perturbative form factor $f_+(t)$, which is estimated through light-cone sum rules [69–71] or lattice simulations [72, 73]. The inclusive measurement requires the use of stringent experimental cuts to suppress the $\mathrm{b} \to \mathrm{X_c}\ell\nu_\ell$ background; this induces large errors in the theoretical predictions [34, 74–81], which become sensitive to non-perturbative shape functions and depend much more strongly on $m_{\rm b}$. The PDG quotes the value [13]

$$|\mathbf{V}_{\rm ub}| \,=\, \left\{ \begin{array}{ll} (3.38 \pm 0.36) \times 10^{-3} & \quad ({\rm B} \to \pi \ell \bar{\nu}_\ell) \\ (4.27 \pm 0.38) \times 10^{-3} & \quad ({\rm B} \to {\rm X_u} \ell \bar{\nu}_\ell) \end{array} \right. \;=\; (3.89 \pm 0.44) \times 10^{-3} , \qquad (31)$$

where the average includes an error scaling factor $\sqrt{\chi^2/\mathrm{dof}} = 1.62$.

4.3 Determination of the charm and top CKM elements

The analytic control of theoretical uncertainties is more difficult in semileptonic charm decays, because the symmetry arguments associated with the light- and heavy-quark limits get corrected by sizeable symmetry-breaking effects. The magnitudes of $|\mathbf{V}_{\rm cd}|$ and $|\mathbf{V}_{\rm cs}|$ can be extracted from $\mathrm{D} \to \pi\ell\nu_\ell$ and $\mathrm{D} \to \mathrm{K}\ell\nu_\ell$ decays. Using the lattice determination of $f_+^{\mathrm{D}\to\pi/\mathrm{K}}(0)$ [82, 83], the CLEO-c [84] measurements of these decays imply [85]

$$|\mathbf{V}_{\rm cd}| \,=\, 0.234 \pm 0.026 \, , \qquad\qquad |\mathbf{V}_{\rm cs}| \,=\, 0.963 \pm 0.026 \, , \qquad (32)$$

where the errors are dominated by lattice uncertainties.

The most precise determination of $|\mathbf{V}_{\rm cd}|$ is based on neutrino and antineutrino interactions. The difference of the ratio of double-muon to single-muon production by neutrino and antineutrino beams is proportional to the charm cross-section off valence d quarks and, therefore, to $|\mathbf{V}_{\rm cd}|$ times the average semileptonic branching ratio of charm mesons. Averaging data from several experiments, the PDG quotes [13]

$$|\mathbf{V}_{\rm cd}| \,=\, 0.230 \pm 0.011 \, . \qquad (33)$$

The analogous determination of $|\mathbf{V}_{cs}|$ from $\nu s \to cX$ suffers from the uncertainty of the s-quark sea content.

The top quark has only been seen decaying into bottom. From the ratio of branching fractions, $\mathrm{Br}(t \to Wb)/\mathrm{Br}(t \to Wq)$, one determines [86, 87]

$$\frac{|\mathbf{V}_{tb}|}{\sqrt{\sum_q |\mathbf{V}_{tq}|^2}} \; > \; 0.89 \quad (95\% \text{ CL}), \tag{34}$$

where $q = \mathrm{b, s, d}$. A more direct determination of $|\mathbf{V}_{tb}|$ can be obtained from the single top-quark production cross-section, measured by D0 [88] and CDF [89]:

$$|\mathbf{V}_{tb}| \; = \; 0.88 \pm 0.07. \tag{35}$$

4.4 Structure of the CKM matrix

Using the previous determinations of CKM elements, we can check the unitarity of the quark-mixing matrix. The most precise test involves the elements of the first row:

$$|\mathbf{V}_{ud}|^2 + |\mathbf{V}_{us}|^2 + |\mathbf{V}_{ub}|^2 \; = \; 1.0000 \pm 0.0007\,, \tag{36}$$

where we have taken as reference values the determinations in Eqs. (24), (26) and (31). Radiative corrections play a crucial role at the quoted level of uncertainty, while the $|\mathbf{V}_{ub}|^2$ contribution is negligible.

The ratio of the total hadronic decay width of the W to the leptonic one provides the sum [90, 91]

$$\sum_{j\,=\,\mathrm{d,s,b}} \left(|\mathbf{V}_{uj}|^2 + |\mathbf{V}_{cj}|^2\right) \; = \; 2.002 \pm 0.027\,. \tag{37}$$

Although much less precise than Eq. (36), this result tests unitarity at the 1.3% level. From Eq. (37) one can also obtain a tighter determination of $|\mathbf{V}_{cs}|$, using the experimental knowledge on the other CKM matrix elements, i.e. $|\mathbf{V}_{ud}|^2 + |\mathbf{V}_{us}|^2 + |\mathbf{V}_{ub}|^2 + |\mathbf{V}_{cd}|^2 + |\mathbf{V}_{cb}|^2 = 1.0546 \pm 0.0051$. This gives

$$|\mathbf{V}_{cs}| \; = \; 0.973 \pm 0.014\,, \tag{38}$$

which is more accurate than the direct determination in Eq. (32).

The measured entries of the CKM matrix show a hierarchical pattern, with the diagonal elements being very close to unity, those connecting the first two generations having a size

$$\lambda \approx |\mathbf{V}_{us}| = 0.2255 \pm 0.0013\,, \tag{39}$$

the mixing between the second and third families being of order λ^2, and the mixing between the first and third quark generations having a much smaller size of about λ^3. It is then quite practicable to use the approximate parametrization [92]:

$$\mathbf{V} \; = \; \begin{bmatrix} 1-\frac{1}{2}\lambda^2 & \lambda & A\lambda^3(\rho - i\eta) \\ -\lambda & 1-\frac{1}{2}\lambda^2 & A\lambda^2 \\ A\lambda^3(1-\rho-i\eta) & -A\lambda^2 & 1 \end{bmatrix} \; + \; O\!\left(\lambda^4\right)\,, \tag{40}$$

where

$$A \approx \frac{|\mathbf{V}_{cb}|}{\lambda^2} = 0.802 \pm 0.024\,, \qquad \sqrt{\rho^2+\eta^2} \approx \left|\frac{\mathbf{V}_{ub}}{\lambda \mathbf{V}_{cb}}\right| \; = 0.423 \pm 0.049\,. \tag{41}$$

Defining to all orders in λ [93] $s_{12} \equiv \lambda$, $s_{23} \equiv A\lambda^2$ and $s_{13}\, e^{-i\delta_{13}} \equiv A\lambda^3(\rho - i\eta)$, Eq. (40) just corresponds to a Taylor expansion of Eq. (11) in powers of λ.

5 Meson–antimeson mixing

Additional information on the CKM parameters can be obtained from flavour-changing neutral-current transitions, occurring at the one-loop level. An important example is provided by the mixing between the B^0 meson and its antiparticle. This process occurs through the box diagrams shown in Fig. 4, where two W bosons are exchanged between a pair of quark lines. The mixing amplitude is proportional to

$$\langle \bar{\mathrm{B}}^0_{\mathrm{d}} | \mathcal{H}_{\Delta B=2} | \mathrm{B}_0 \rangle \;\sim\; \sum_{ij} \mathbf{V}_{i\mathrm{d}} \mathbf{V}^*_{i\mathrm{b}} \mathbf{V}_{j\mathrm{d}} \mathbf{V}^*_{j\mathrm{b}}\, S(r_i, r_j) \;\sim\; \mathbf{V}^2_{\mathrm{td}}\, S(r_{\mathrm{t}}, r_{\mathrm{t}}), \tag{42}$$

where $S(r_i, r_j)$ is a loop function [94] that depends on the masses ($r_i \equiv m_i^2/M_{\mathrm{W}}^2$) of the up-type quarks running along the internal fermionic lines. Owing to the unitarity of the CKM matrix, the mixing vanishes for equal (up-type) quark masses (GIM mechanism [7]); thus the effect is proportional to the mass splittings between the u, c and t quarks. Since the different CKM factors have all a similar size, $\mathbf{V}_{\mathrm{ud}}\mathbf{V}^*_{\mathrm{ub}} \sim \mathbf{V}_{\mathrm{cd}}\mathbf{V}^*_{\mathrm{cb}} \sim \mathbf{V}_{\mathrm{td}}\mathbf{V}^*_{\mathrm{tb}} \sim A\lambda^3$, the final amplitude is completely dominated by the top contribution. This transition can then be used to perform an indirect determination of $\mathbf{V}_{\mathrm{td}}$.

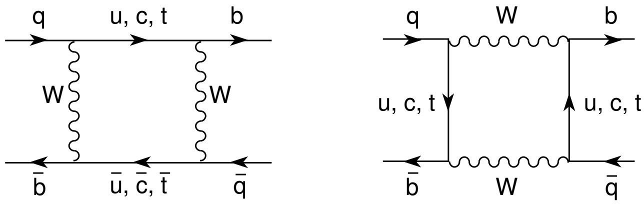

Fig. 4: Box diagrams contributing to B^0–$\bar{\mathrm{B}}^0$ mixing.

Note that this determination has a qualitatively different character than those obtained before from tree-level weak decays. Now, we are going to test the structure of the electroweak theory at the quantum level. This flavour-changing transition could then be sensitive to contributions from new physics at higher energy scales. Moreover, the mixing amplitude crucially depends on the unitarity of the CKM matrix. Without the GIM mechanism embodied in the CKM mixing structure, the calculation of the analogous $\mathrm{K}^0 \to \bar{\mathrm{K}}^0$ transition (replace the b quark by a s in the box diagrams) would have failed to explain the observed K^0–$\bar{\mathrm{K}}^0$ mixing by several orders of magnitude [95].

5.1 General Formalism

Since weak interactions can transform a P^0 state ($P = \mathrm{K}, \mathrm{D}, \mathrm{B}$) into its antiparticle $\bar{P}^0$, these flavour eigenstates are not mass eigenstates and do not follow an exponential decay law. Let us consider an arbitrary mixture of the two flavour states,

$$|\psi(t)\rangle \;=\; a(t)\,|P^0\rangle + b(t)\,|\bar{P}^0\rangle \;\equiv\; \begin{pmatrix} a(t) \\ b(t) \end{pmatrix}, \tag{43}$$

with the time evolution

$$\mathrm{i}\,\frac{\mathrm{d}}{\mathrm{d}t}\,|\psi(t)\rangle \;=\; \mathcal{M}\,|\psi(t)\rangle\,. \tag{44}$$

Assuming CPT symmetry to hold, the 2×2 mixing matrix can be written as

$$\mathcal{M} = \begin{pmatrix} M & M_{12} \\ M^*_{12} & M \end{pmatrix} - \frac{\mathrm{i}}{2} \begin{pmatrix} \Gamma & \Gamma_{12} \\ \Gamma^*_{12} & \Gamma \end{pmatrix}. \tag{45}$$

The diagonal elements M and Γ are real parameters, which would correspond to the mass and width of the neutral mesons in the absence of mixing. The off-diagonal entries contain the *dispersive* and *absorptive* parts of the $\Delta P = 2$ transition amplitude. If CP were an exact symmetry, M_{12} and Γ_{12} would also be real. The physical eigenstates of $\mathcal{M}$ are

$$|P_\mp\rangle \;=\; \frac{1}{\sqrt{|p|^2+|q|^2}}\;\left[p\,|P^0\rangle\;\mp\;q\,|\bar{P}^0\rangle\right], \qquad (46)$$

with

$$\frac{q}{p}\;\equiv\;\frac{1-\bar{\varepsilon}}{1+\bar{\varepsilon}}\;=\;\left(\frac{M_{12}^*-\frac{1}{2}\mathrm{i}\Gamma_{12}^*}{M_{12}-\frac{1}{2}\mathrm{i}\Gamma_{12}}\right)^{1/2}. \qquad (47)$$

If M_{12} and Γ_{12} were real, then $q/p = 1$ and $|\mathrm{B}_\mp\rangle$ would correspond to the CP-even and CP-odd states (we use the phase convention[3] $\mathrm{CP}|P^0\rangle = -|\bar{P}^0\rangle$)

$$|P_{1,2}\rangle \equiv \frac{1}{\sqrt{2}}(|P^0\rangle \mp |\bar{P}^0\rangle), \qquad \mathrm{CP}\,|P_{1,2}\rangle = \pm|P_{1,2}\rangle. \qquad (48)$$

The two mass eigenstates are no longer orthogonal when CP is violated:

$$\langle P_-|P_+\rangle \;=\; \frac{|p|^2-|q|^2}{|p|^2+|q|^2}\;=\;\frac{2\,\mathrm{Re}(\bar{\varepsilon})}{(1+|\bar{\varepsilon}|^2)}. \qquad (49)$$

The time evolution of a state that was originally produced as a P^0 or a $\bar{P}^0$ is given by

$$\begin{pmatrix} |P^0(t)\rangle \\ |\bar{P}^0(t)\rangle \end{pmatrix} \;=\; \begin{pmatrix} g_1(t) & (q/p)g_2(t) \\ (p/q)g_2(t) & g_1(t) \end{pmatrix} \begin{pmatrix} |P^0\rangle \\ |\bar{P}^0\rangle \end{pmatrix}, \qquad (50)$$

where

$$\begin{pmatrix} g_1(t) \\ g_2(t) \end{pmatrix} \;=\; \mathrm{e}^{-\mathrm{i}Mt}\,\mathrm{e}^{-\Gamma t/2} \begin{pmatrix} \cos\left[(\Delta M - \frac{1}{2}\mathrm{i}\Delta\Gamma)t/2\right] \\ -\mathrm{i}\sin\left[(\Delta M - \frac{1}{2}\mathrm{i}\Delta\Gamma)t/2\right] \end{pmatrix}, \qquad (51)$$

with

$$\Delta M \equiv M_{P_+} - M_{P_-}, \qquad \Delta\Gamma \equiv \Gamma_{P_+} - \Gamma_{P_-}. \qquad (52)$$

5.2 Experimental measurements

The main difference between the K^0–$\bar{\mathrm{K}}^0$ and B^0–$\bar{\mathrm{B}}^0$ systems stems from the different kinematics involved. The light kaon mass only allows the hadronic decay modes $\mathrm{K}^0 \to 2\pi$ and $\mathrm{K}^0 \to 3\pi$. Since $\mathrm{CP}|\pi\pi\rangle = +|\pi\pi\rangle$, the CP-even kaon state decays into 2π whereas the CP-odd one decays into the phase-space-suppressed 3π mode. Therefore, there is a large lifetime difference and we have a short-lived $|\mathrm{K}_S\rangle \equiv |\mathrm{K}_-\rangle \approx |\mathrm{K}_1\rangle + \bar{\varepsilon}_\mathrm{K}|\mathrm{K}_2\rangle$ and a long-lived $|\mathrm{K}_L\rangle \equiv |\mathrm{K}_+\rangle \approx |\mathrm{K}_2\rangle + \bar{\varepsilon}_\mathrm{K}|\mathrm{K}_1\rangle$ kaon, with $\Gamma_{\mathrm{K}_L} \ll \Gamma_{\mathrm{K}_S}$. One finds experimentally that $\Delta\Gamma_{\mathrm{K}^0} \approx -\Gamma_{\mathrm{K}_S} \approx -2\Delta M_{\mathrm{K}^0}$ [13]:

$$\Delta M_{\mathrm{K}^0} = (0.5292 \pm 0.0009) \times 10^{10}\ \mathrm{s}^{-1}, \qquad \Delta\Gamma_{\mathrm{K}^0} = -(1.1150 \pm 0.0006) \times 10^{10}\ \mathrm{s}^{-1}. \qquad (53)$$

In the B system, there are many open decay channels and a large part of them are common to both mass eigenstates. Therefore, the $|\mathrm{B}_\mp\rangle$ states have a similar lifetime; i.e. $|\Delta\Gamma_{\mathrm{B}^0}| \ll \Gamma_{\mathrm{B}^0}$. Moreover, whereas the B^0–$\bar{\mathrm{B}}^0$ transition is dominated by the top box diagram, the decay amplitudes obviously get their main contribution from the $\mathrm{b} \to \mathrm{c}$ process. Thus, $|\Delta\Gamma_{\mathrm{B}^0}/\Delta M_{\mathrm{B}^0}| \sim m_\mathrm{b}^2/m_\mathrm{t}^2 \ll 1$. To measure the mixing transition experimentally requires the identification of the B-meson flavour at both

[3] Since flavour is conserved by strong interactions, there is some freedom in defining the phases of flavour eigenstates. One could use $|P^0_\zeta\rangle \equiv \mathrm{e}^{-\mathrm{i}\zeta}|P^0\rangle$ and $|\bar{P}^0_\zeta\rangle \equiv \mathrm{e}^{\mathrm{i}\zeta}|\bar{P}^0\rangle$, which satisfy $\mathrm{CP}\,|P^0_\zeta\rangle = -\mathrm{e}^{-2\mathrm{i}\zeta}|\bar{P}^0_\zeta\rangle$. The two bases are trivially related: $M^\zeta_{12} = \mathrm{e}^{2\mathrm{i}\zeta}M_{12}$, $\Gamma^\zeta_{12} = \mathrm{e}^{2\mathrm{i}\zeta}\Gamma_{12}$ and $(q/p)_\zeta = \mathrm{e}^{-2\mathrm{i}\zeta}(q/p)$. Thus, $q/p \neq 1$ does not necessarily imply CP-violation. CP is violated if $|q/p| \neq 1$; i.e. $\mathrm{Re}(\bar{\varepsilon}) \neq 0$ and $\langle P_-|P_+\rangle \neq 0$. Note that $\langle P_-|P_+\rangle_\zeta = \langle P_-|P_+\rangle$. Another phase-convention-independent quantity is $(q/p)\,(\bar{A}_f/A_f)$, where $A_f \equiv A(P^0\to f)$ and $\bar{A}_f \equiv -A(\bar{P}^0\to f)$, for any final state f.

its production and decay time. This can be done through flavour-specific decays such as $\mathrm{B}^0 \to \mathrm{X}\ell^+\nu_\ell$ and $\bar{\mathrm{B}}^0 \to \mathrm{X}\ell^-\bar{\nu}_\ell$. In general, mixing is measured by studying pairs of B mesons so that one B can be used to *tag* the initial flavour of the other meson. For instance, in $\mathrm{e}^+\mathrm{e}^-$ machines, one can look into the pair production process $\mathrm{e}^+\mathrm{e}^- \to \mathrm{B}^0\bar{\mathrm{B}}^0 \to (\mathrm{X}\ell\nu_\ell)\,(\mathrm{Y}\ell\nu_\ell)$. In the absence of mixing, the final leptons should have opposite charges; the amount of like-sign leptons is then a clear signature of meson mixing.

Evidence for a large B^0_d–$\bar{\mathrm{B}}^0_\mathrm{d}$ mixing was first reported in 1987 by ARGUS [96]. This provided the first indication that the top quark was very heavy. Since then, many experiments have analysed the mixing probability. The present world-average value is [13, 57]:

$$\Delta M_{\mathrm{B}^0_\mathrm{d}} = (0.507 \pm 0.004) \times 10^{12}\ \mathrm{s}^{-1}, \qquad x_{\mathrm{B}^0_\mathrm{d}} \equiv \frac{\Delta M_{\mathrm{B}^0_\mathrm{d}}}{\Gamma_{\mathrm{B}^0_\mathrm{d}}} = 0.771 \pm 0.008. \tag{54}$$

The first direct evidence of B^0_s–$\bar{\mathrm{B}}^0_\mathrm{s}$ oscillations was obtained by CDF [97]. The large measured mass difference reflects the CKM hierarchy $|\mathbf{V}_{\mathrm{ts}}|^2 \gg |\mathbf{V}_{\mathrm{td}}|^2$, implying very fast oscillations [13, 57]:

$$\Delta M_{\mathrm{B}^0_\mathrm{s}} = (17.77 \pm 0.12) \times 10^{12}\ \mathrm{s}^{-1}, \qquad x_{\mathrm{B}^0_\mathrm{s}} \equiv \frac{\Delta M_{\mathrm{B}^0_\mathrm{s}}}{\Gamma_{\mathrm{B}^0_\mathrm{s}}} = 26.2 \pm 0.5. \tag{55}$$

A more precise but still preliminary value, $\Delta M_{\mathrm{B}^0_\mathrm{s}} = (17.725 \pm 0.041 \pm 0.026)\ \mathrm{ps}^{-1}$, has recently been obtained by LHCb [98] using the flavour-specific decays $\mathrm{B}^0_\mathrm{s} \to \mathrm{D}^-_\mathrm{s}\pi^+$ and $\bar{\mathrm{B}}^0_\mathrm{s} \to \mathrm{D}^+_\mathrm{s}\pi^-$.

Evidence of mixing has also been obtained in the D_0–$\bar{\mathrm{D}}_0$ system. The present world averages [57],

$$x_{\mathrm{D}_0} \equiv \frac{\Delta M_{\mathrm{D}_0}}{\Gamma_{\mathrm{D}_0}} = -(0.63\,^{+0.19}_{-0.20})\%, \qquad y_{\mathrm{D}_0} \equiv \frac{\Delta\Gamma_{\mathrm{D}_0}}{2\Gamma_{\mathrm{D}_0}} = -(0.75 \pm 0.12)\%, \tag{56}$$

confirm the SM expectation of a very slow oscillation, compared with the decay rate.

5.3 Mixing constraints on the CKM matrix

Long-distance contributions arising from intermediate hadronic states completely dominate the D_0–$\bar{\mathrm{D}}_0$ mixing amplitude and are very sizeable in the K_0–$\bar{\mathrm{K}}_0$ case, making it difficult to extract useful information on the CKM matrix. The situation is much better for B^0 mesons, owing to the dominance of the short-distance top contribution, which is known to next-to-leading-order (NLO) in the strong coupling [99, 100]. The main uncertainty stems from the hadronic matrix element of the $\Delta B = 2$ four-quark operator

$$\langle \bar{\mathrm{B}}^0 \,|\, (\bar{\mathrm{b}}\gamma^\mu(1-\gamma_5)\mathrm{d})\,(\bar{\mathrm{b}}\gamma_\mu(1-\gamma_5)\mathrm{d})\,|\,\mathrm{B}^0\rangle \;\equiv\; \tfrac{8}{3}\, M_\mathrm{B}^2\, \xi_\mathrm{B}^2, \tag{57}$$

which is characterized through the non-perturbative parameter [101] $\xi_\mathrm{B}(\mu) \equiv \sqrt{2}\, f_\mathrm{B} \sqrt{B_\mathrm{B}(\mu)}$. Present lattice calculations obtain the ranges [102] $\hat{\xi}_{\mathrm{B_d}} = (216 \pm 15)$ MeV, $\hat{\xi}_{\mathrm{B_s}} = (266 \pm 18)$ MeV and $\hat{\xi}_{\mathrm{B_s}}/\hat{\xi}_{\mathrm{B_d}} = 1.258 \pm 0.033$, where $\hat{\xi}_\mathrm{B} \approx \alpha_s(\mu)^{-3/23}\xi_\mathrm{B}(\mu)$ is the corresponding renormalization-group-invariant quantity. Using these values, the measured mixings in (54) and (55) imply

$$|\mathbf{V}^*_{\mathrm{tb}}\mathbf{V}_{\mathrm{td}}| \;=\; 0.0084 \pm 0.0006\,, \qquad |\mathbf{V}^*_{\mathrm{tb}}\mathbf{V}_{\mathrm{ts}}| \;=\; 0.040 \pm 0.003\,, \qquad \frac{|\mathbf{V}_{\mathrm{td}}|}{|\mathbf{V}_{\mathrm{ts}}|} \;=\; 0.214 \pm 0.006\,. \tag{58}$$

The last number takes advantage of the smaller uncertainty in the ratio $\hat{\xi}_{\mathrm{B_s}}/\hat{\xi}_{\mathrm{B_d}}$. Since $|\mathbf{V}_{\mathrm{tb}}| \approx 1$, $\mathrm{B}^0_{\mathrm{d,s}}$ mixing provides indirect determinations of $|\mathbf{V}_{\mathrm{td}}|$ and $|\mathbf{V}_{\mathrm{ts}}|$. The resulting value of $|\mathbf{V}_{\mathrm{ts}}|$ is in perfect agreement with Eq. (30), satisfying the unitarity constraint $|\mathbf{V}_{\mathrm{ts}}| \approx |\mathbf{V}_{\mathrm{cb}}|$. In terms of the (ρ, η) parametrization of Eq. (40), one obtains

$$\sqrt{(1-\rho)^2 + \eta^2} \;=\; \begin{cases} \left|\dfrac{\mathbf{V}_{\mathrm{td}}}{\lambda\mathbf{V}_{\mathrm{cb}}}\right| \;=\; 0.91 \pm 0.07, \\[2ex] \left|\dfrac{\mathbf{V}_{\mathrm{td}}}{\lambda\mathbf{V}_{\mathrm{ts}}}\right| \;=\; 0.95 \pm 0.03. \end{cases} \tag{59}$$

The uncertainties in all these determinations are dominated by the theoretical errors on the hadronic matrix elements. Therefore, they are not improved by the recent precise LHCb measurement of $\Delta M_{\mathrm{B}^0_\mathrm{s}}$.

6 CP-violation

While parity and charge conjugation are violated by the weak interactions in a maximal way, the product of the two discrete transformations is still a good symmetry of the gauge interactions (left-handed fermions $\longleftrightarrow$ right-handed antifermions). In fact, CP appears to be a symmetry of nearly all observed phenomena. However, a slight violation of the CP symmetry at the level of 0.2% is observed in the neutral kaon system and more sizeable signals of CP-violation have been established at the B factories. Moreover, the huge matter–antimatter asymmetry present in our Universe is a clear manifestation of CP-violation and its important role in the primordial baryogenesis.

The CPT theorem guarantees that the product of the three discrete transformations is an exact symmetry of any local and Lorentz-invariant quantum field theory preserving microcausality. A violation of CP thus requires a corresponding violation of time reversal. Since $\mathcal{T}$ is an anti-unitary transformation, this requires the presence of relatively complex phases between different interfering amplitudes.

The electroweak SM Lagrangian only contains a single complex phase δ_{13} (η). This is the sole possible source of CP-violation and, therefore, the SM predictions for CP-violating phenomena are quite constrained. The CKM mechanism requires several necessary conditions in order to generate an observable CP-violation effect. With only two fermion generations, the quark-mixing mechanism cannot give rise to CP-violation; therefore, for CP-violation to occur in a particular process, all three generations are required to play an active role. In the kaon system, for instance, CP-violation can only appear at the one-loop level, where the top quark is present. In addition, all CKM matrix elements must be non-zero and the quarks of a given charge must be non-degenerate in mass. If any of these conditions were not satisfied, the CKM phase could be rotated away by a redefinition of the quark fields. CP-violation effects are then necessarily proportional to the product of all CKM angles, and should vanish in the limit where any two (equal-charge) quark masses are taken to be equal. All these necessary conditions can be summarized as a single requirement on the original quark mass matrices $\mathbf{M}'_{\mathrm{u}}$ and $\mathbf{M}'_{\mathrm{d}}$ [103]:

$$\text{CP violation} \qquad \Longleftrightarrow \qquad \mathrm{Im}\{\det[\mathbf{M}'_{\mathrm{u}}\mathbf{M}'^{\dagger}_{\mathrm{u}}, \mathbf{M}'_{\mathrm{d}}\mathbf{M}'^{\dagger}_{\mathrm{d}}]\} \neq 0. \tag{60}$$

Without performing any detailed calculation, one can make the following general statements on the implications of the CKM mechanism of CP-violation:

– Owing to unitarity, for any choice of i, j, k, l (between 1 and 3),

$$\mathrm{Im}[\mathbf{V}_{ij}\mathbf{V}^*_{ik}\mathbf{V}_{lk}\mathbf{V}^*_{lj}] = \mathcal{J} \sum_{m,n=1}^{3} \epsilon_{ilm}\epsilon_{jkn}, \tag{61}$$

$$\mathcal{J} = c_{12}c_{23}c_{13}^2 s_{12}s_{23}s_{13}\sin\delta_{13} \approx A^2\lambda^6\eta < 10^{-4}. \tag{62}$$

Any CP-violation observable involves the product $\mathcal{J}$ [103]. Thus, violations of the CP symmetry are necessarily small.

– In order to have sizeable CP-violating asymmetries $\mathcal{A} \equiv (\Gamma - \overline{\Gamma})/(\Gamma + \overline{\Gamma})$, one should look for very suppressed decays, where the decay widths already involve small CKM matrix elements.

– In the SM, CP-violation is a low-energy phenomenon, in the sense that any effect should disappear when the quark mass difference $m_{\mathrm{c}} - m_{\mathrm{u}}$ becomes negligible.

– B decays are the optimal place for CP-violation signals to show up. They involve small CKM matrix elements and are the lowest-mass processes where the three quark generations play a direct (tree-level) role.

The SM mechanism of CP-violation is based on the unitarity of the CKM matrix. Testing the constraints implied by unitarity is then a way to test the source of CP-violation. The unitarity tests in

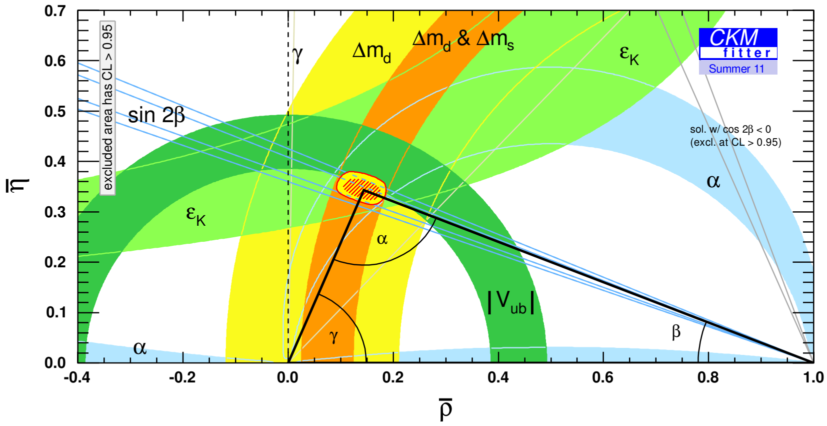

Fig. 5: Experimental constraints on the SM unitarity triangle [104].

Eqs. (36) and (37) involve only the moduli of the CKM parameters, while CP-violation has to do with their phases. More interesting are the off-diagonal unitarity conditions:

$$\begin{aligned} \mathbf{V}_{\rm ud}^*\mathbf{V}_{\rm us} + \mathbf{V}_{\rm cd}^*\mathbf{V}_{\rm cs} + \mathbf{V}_{\rm td}^*\mathbf{V}_{\rm ts} &= 0\,, \\ \mathbf{V}_{\rm us}^*\mathbf{V}_{\rm ub} + \mathbf{V}_{\rm cs}^*\mathbf{V}_{\rm cb} + \mathbf{V}_{\rm ts}^*\mathbf{V}_{\rm tb} &= 0\,, \\ \mathbf{V}_{\rm ub}^*\mathbf{V}_{\rm ud} + \mathbf{V}_{\rm cb}^*\mathbf{V}_{\rm cd} + \mathbf{V}_{\rm tb}^*\mathbf{V}_{\rm td} &= 0\,. \end{aligned} \tag{63}$$

These relations can be visualized by triangles in a complex plane that, owing to Eq. (61), have the same area $|\mathcal{J}|/2$. In the absence of CP-violation, these triangles would degenerate into segments along the real axis.

In the first two triangles, one side is much shorter than the other two (the Cabibbo suppression factors of the three sides are λ, λ and λ^5 in the first triangle, and λ^4, λ^2 and λ^2 in the second one). This is why CP effects are so small for K mesons (first triangle), and why certain asymmetries in $\mathrm{B_s}$ decays are predicted to be tiny (second triangle). The third triangle looks more interesting, since the three sides have a similar size of about λ^3. They are small, which means that the relevant b-decay branching ratios are small, but once enough B mesons have been produced, the CP-violation asymmetries are sizeable. The present experimental constraints on this triangle are shown in Fig. 5, where it has been scaled by dividing its sides by $\mathbf{V}_{\rm cb}^*\mathbf{V}_{\rm cd}$. This aligns one side of the triangle along the real axis and makes its length equal to 1; the coordinates of the three vertices are then $(0,0)$, $(1,0)$ and $(\bar\rho,\bar\eta) \approx (1-\lambda^2/2)\,(\rho,\eta)$.

We have already determined the sides of the unitarity triangle in Eqs. (41) and (59), through two CP-conserving observables: $|\mathbf{V}_{\rm ub}/\mathbf{V}_{\rm cb}|$ and $\mathrm{B}^0_{\rm d,s}$ mixing. This gives the circular regions shown in Fig. 5, centered at the vertices $(0,0)$ and $(1,0)$. Their overlap at $\eta \neq 0$ establishes that CP is violated (assuming unitarity). More direct constraints on the parameter η can be obtained from CP-violating observables, which provide sensitivity to the angles of the unitarity triangle ($\alpha+\beta+\gamma=\pi$):

$$\alpha \equiv \arg\left[-\frac{\mathbf{V}_{\rm td}\mathbf{V}_{\rm tb}^*}{\mathbf{V}_{\rm ud}\mathbf{V}_{\rm ub}^*}\right], \qquad \beta \equiv \arg\left[-\frac{\mathbf{V}_{\rm cd}\mathbf{V}_{\rm cb}^*}{\mathbf{V}_{\rm td}\mathbf{V}_{\rm tb}^*}\right], \qquad \gamma \equiv \arg\left[-\frac{\mathbf{V}_{\rm ud}\mathbf{V}_{\rm ub}^*}{\mathbf{V}_{\rm cd}\mathbf{V}_{\rm cb}^*}\right]. \tag{64}$$

6.1 Indirect and direct CP-violation in the kaon system

Any observable CP-violation effect is generated by the interference between different amplitudes contributing to the same physical transition. This interference can occur either through meson–antimeson mixing or via final-state interactions, or by a combination of both effects.

The flavour-specific decays $\mathrm{K}_0 \to \pi^-\ell^+\nu_\ell$ and $\bar{\mathrm{K}}_0 \to \pi^+\ell^-\bar\nu_\ell$ provide a way to measure the departure of the K_0–$\bar{\mathrm{K}}_0$ mixing parameter $|p/q|$ from unity. In the SM, the decay amplitudes satisfy

$|A(\bar{K}_0 \to \pi^+\ell^-\bar{\nu}_\ell)| = |A(K_0 \to \pi^-\ell^+\nu_\ell)|$ and therefore

$$\delta_L \equiv \frac{\Gamma(K_L \to \pi^-\ell^+\nu_\ell) - \Gamma(K_L \to \pi^+\ell^-\bar{\nu}_\ell)}{\Gamma(K_L \to \pi^-\ell^+\nu_\ell) + \Gamma(K_L \to \pi^+ l^-\bar{\nu}_\ell)} = \frac{|p|^2 - |q|^2}{|p|^2 + |q|^2} = \frac{2\,\mathrm{Re}(\bar{\varepsilon}_K)}{(1 + |\bar{\varepsilon}_K|^2)} \,. \tag{65}$$

The experimental measurement [13], $\delta_L = (3.32 \pm 0.06) \times 10^{-3}$, implies

$$\mathrm{Re}(\bar{\varepsilon}_K) = (1.66 \pm 0.03) \times 10^{-3} \,, \tag{66}$$

which establishes the presence of *indirect* CP-violation generated by the mixing amplitude.

If the flavour of the decaying meson P is known, any observed difference between the decay rate $\Gamma(P \to f)$ and its CP conjugate $\Gamma(\bar{P} \to \bar{f})$ would indicate that CP is directly violated in the decay amplitude. One could study, for instance, CP asymmetries in decays such as $K^\pm \to \pi^\pm\pi^0$ where the pion charges identify the kaon flavour; no positive signal has been found in charged kaon decays. Since at least two interfering contributions are needed, let us write the decay amplitudes as

$$A[P \to f] = M_1\, e^{i\phi_1}\, e^{i\delta_1} + M_2\, e^{i\phi_2}\, e^{i\delta_2} \,, \qquad A[\bar{P} \to \bar{f}] = M_1\, e^{-i\phi_1} e^{i\delta_1} + M_2\, e^{-i\phi_2} e^{i\delta_2} \,, \tag{67}$$

where ϕ_i denote weak phases, δ_i strong final-state phases and M_i the moduli of the matrix elements. The rate asymmetry is given by

$$\mathcal{A}^{CP}_{P\to f} \equiv \frac{\Gamma[P \to f] - \Gamma[\bar{P} \to \bar{f}]}{\Gamma[P \to f] + \Gamma[\bar{P} \to \bar{f}]} = \frac{-2M_1M_2\, \sin(\phi_1 - \phi_2)\, \sin(\delta_1 - \delta_2)}{|M_1|^2 + |M_2|^2 + 2M_1M_2\, \cos(\phi_1 - \phi_2)\, \cos(\delta_1 - \delta_2)} \,. \tag{68}$$

Thus, to generate a direct CP asymmetry one needs: (i) at least two interfering amplitudes, which should be of comparable size in order to get a sizeable asymmetry; (ii) two different weak phases $[\sin(\phi_1 - \phi_2) \neq 0]$; and (iii) two different strong phases $[\sin(\delta_1 - \delta_2) \neq 0]$.

Direct CP-violation has been sought in decays of neutral kaons, where K_0–$\bar{K}_0$ mixing is also involved. Thus, both direct and indirect CP-violation need to be taken into account simultaneously. A CP-violation signal is provided by the ratios:

$$\eta_{+-} \equiv \frac{A(K_L \to \pi^+\pi^-)}{A(K_S \to \pi^+\pi^-)} = \varepsilon_K + \varepsilon'_K \,, \qquad \eta_{00} \equiv \frac{A(K_L \to \pi^0\pi^0)}{A(K_S \to \pi^0\pi^0)} = \varepsilon_K - 2\varepsilon'_K \,. \tag{69}$$

The dominant effect from CP-violation in K_0–$\bar{K}^0$ mixing is contained in ε_K, while ε'_K accounts for direct CP-violation in the decay amplitudes:

$$\varepsilon_K = \bar{\varepsilon}_K + i\xi_0, \qquad \varepsilon'_K = \frac{i}{\sqrt{2}}\,\omega\,(\xi_2 - \xi_0) \,, \qquad \omega \equiv \frac{\mathrm{Re}(A_2)}{\mathrm{Re}(A_0)}\, e^{i(\delta_2 - \delta_0)} \,, \qquad \xi_I \equiv \frac{\mathrm{Im}(A_I)}{\mathrm{Re}(A_I)} \,. \tag{70}$$

Here A_I and δ_I are the decay amplitudes and strong phase shifts of isospin $I = 0, 2$ (these are the only two values allowed by Bose symmetry for the final 2π state). Although ε'_K is strongly suppressed by the small ratio $|\omega| \approx 1/22$ [44], a non-zero value has been established through very accurate measurements, demonstrating the existence of direct CP-violation in K decays [105–108]:

$$\mathrm{Re}(\varepsilon'_K/\varepsilon_K) = \frac{1}{3}\left(1 - \left|\frac{\eta_{00}}{\eta_{+-}}\right|\right) = (16.8 \pm 1.4) \times 10^{-4} \,. \tag{71}$$

In the SM the necessary weak phases are generated through the gluonic and electroweak penguin diagrams shown in Fig. 6, involving virtual up-type quarks of the three generations in the loop. These short-distance contributions are known to NLO in the strong coupling [109, 110]. However, the theoretical prediction involves a delicate balance between the two isospin amplitudes and is sensitive to long-distance and isospin-violating effects. Using chiral perturbation theory techniques [111–113], one finds $\mathrm{Re}(\varepsilon'_K/\varepsilon_K) = (19\,^{+11}_{-9}) \times 10^{-4}$ [44], in agreement with (71) but with a large uncertainty.

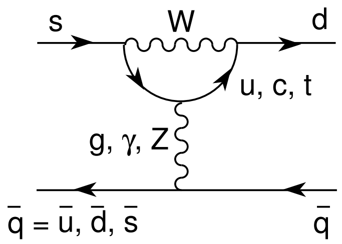

Fig. 6: The $\Delta S = 1$ penguin diagrams.

Since $\mathrm{Re}(\varepsilon'_{\mathrm{K}}/\varepsilon_{\mathrm{K}}) \ll 1$, the ratios η_{+-} and η_{00} provide a measurement of $\varepsilon_{\mathrm{K}} = |\varepsilon_{\mathrm{K}}|\, \mathrm{e}^{\mathrm{i}\phi_\varepsilon}$ [13]:

$$|\varepsilon_{\mathrm{K}}| \,=\, \tfrac{1}{3}(2|\eta_{+-}| + |\eta_{00}|) \,=\, (2.228 \pm 0.011) \times 10^{-3}, \qquad \phi_\varepsilon \,=\, (43.51 \pm 0.05)^\circ\,, \tag{72}$$

in perfect agreement with the semileptonic asymmetry δ_L. In the SM, ε_{K} receives short-distance contributions from box diagrams involving virtual top and charm quarks, which are proportional to

$$\varepsilon_{\mathrm{K}} \,\propto\, \sum_{i,j=\mathrm{c,t}} \eta_{ij}\, \mathrm{Im}[\mathbf{V}_{i\mathrm{d}}\mathbf{V}^*_{i\mathrm{s}}\mathbf{V}_{j\mathrm{d}}\mathbf{V}^*_{j\mathrm{s}}]\, S(r_i, r_j) \,\propto\, A^2\lambda^6\bar{\eta}\{\eta_{\mathrm{tt}}\, A^2\lambda^4(1-\bar{\rho}) + P_{\mathrm{c}}\}. \tag{73}$$

The first term shows the CKM dependence of the dominant top contribution, P_{c} accounts for the charm corrections [114] and the short-distance QCD corrections η_{ij} are known to NLO [99, 100, 115]. The measured value of $|\varepsilon_{\mathrm{K}}|$ determines a hyperbolic constraint in the $(\bar{\rho}, \bar{\eta})$ plane, shown in Fig. 5, taking into account the theoretical uncertainty in the hadronic matrix element of the $\Delta S = 2$ operator [34, 44].

6.2 CP asymmetries in B decays

The semileptonic decays $\mathrm{B}^0 \to \mathrm{X}^-\ell^+\nu_\ell$ and $\bar{\mathrm{B}}^0 \to \mathrm{X}^+\ell^-\bar{\nu}_\ell$ provide the most direct way to measure the amount of CP-violation in the B^0–$\bar{\mathrm{B}}^0$ mixing matrix, through

$$\begin{aligned} a^q_{\mathrm{sl}} \;&\equiv\; \frac{\Gamma(\bar{\mathrm{B}}^0_q \to \mathrm{X}^-\ell^+\nu_\ell) - \Gamma(\mathrm{B}^0_q \to \mathrm{X}^+ l^-\bar{\nu}_\ell)}{\Gamma(\bar{\mathrm{B}}^0_q \to \mathrm{X}^-\ell^+\nu_\ell) + \Gamma(\mathrm{B}^0_q \to \mathrm{X}^+ l^-\bar{\nu}_\ell)} \;=\; \frac{|p|^4 - |q|^4}{|p|^4 + |q|^4} \;\approx\; 4\,\mathrm{Re}(\bar{\varepsilon}_{\mathrm{B}^0_q}) \\ &\approx\; \frac{|\Gamma_{12}|}{|M_{12}|}\,\sin\phi_q \;\approx\; \frac{|\Delta\Gamma_{\mathrm{B}^0_q}|}{|\Delta M_{\mathrm{B}^0_q}|}\,\tan\phi_q. \end{aligned} \tag{74}$$

This asymmetry is expected to be tiny because $|\Gamma_{12}/M_{12}| \sim m_{\mathrm{b}}^2/m_{\mathrm{t}}^2 \ll 1$. Moreover, there is an additional GIM suppression in the relative mixing phase $\phi_q \equiv \arg\left(-M_{12}/\Gamma_{12}\right) \sim (m_{\mathrm{c}}^2 - m_{\mathrm{u}}^2)/m_{\mathrm{b}}^2$, implying a value of $|q/p|$ very close to 1. Therefore, a^q_{sl} could be very sensitive to new CP phases contributing to ϕ_q. The present measurements give [13, 57]

$$\mathrm{Re}(\bar{\varepsilon}_{\mathrm{B}^0_{\mathrm{d}}}) \,=\, (-0.1 \pm 1.4) \times 10^{-3}, \qquad \mathrm{Re}(\bar{\varepsilon}_{\mathrm{B}^0_{\mathrm{s}}}) \,=\, (-2.9 \pm 1.5) \times 10^{-3}. \tag{75}$$

The non-zero value of $\mathrm{Re}(\bar{\varepsilon}_{\mathrm{B}^0_{\mathrm{s}}})$ originates in a recent D0 measurement [116] claiming the like-sign dimuon charge asymmetry to be 3.9σ larger than the SM prediction [117, 118]. However, this is not supported by the measured CP asymmetries in $\mathrm{B}^0_{\mathrm{s}} \to \mathrm{J}/\psi\phi$ [119–121] and $\mathrm{B}^0_{\mathrm{s}} \to \mathrm{J}/\psi f_0(980)$ [119], which are in good agreement with the SM expectations.

The large B^0–$\bar{\mathrm{B}}^0$ mixing provides a different way to generate the required CP-violating interference. There are quite a few non-leptonic final states that are reachable from both B^0 and $\bar{\mathrm{B}}^0$. For these flavour non-specific decays, the B^0 (or $\bar{\mathrm{B}}^0$) can decay directly to the given final state f, or do it after the meson has been changed to its antiparticle via the mixing process; i.e. there are two different amplitudes, $A(\mathrm{B}^0 \to f)$ and $A(\mathrm{B}^0 \to \bar{\mathrm{B}}^0 \to f)$, corresponding to two possible decay paths. CP-violating effects can then result from the interference of these two contributions.

The time-dependent decay probabilities for the decay of a neutral B meson created at the time $t_0 = 0$ as a pure B^0 ($\bar{\mathrm{B}}^0$) into the final state f ($\bar{f} \equiv \mathrm{CP}\, f$) are

$$\Gamma[\mathrm{B}^0(t) \to f] \;\propto\; \tfrac{1}{2}\,\mathrm{e}^{-\Gamma_{\mathrm{B}^0} t}\,(|A_f|^2 + |\bar{A}_f|^2)\,\{1 + C_f\,\cos(\Delta M_{\mathrm{B}^0} t) - S_f\,\sin(\Delta M_{\mathrm{B}^0} t)\},$$
$$\Gamma[\bar{\mathrm{B}}^0(t) \to \bar{f}] \;\propto\; \tfrac{1}{2}\,\mathrm{e}^{-\Gamma_{\mathrm{B}^0} t}\,(|\bar{A}_{\bar{f}}|^2 + |A_{\bar{f}}|^2)\,\{1 - C_{\bar{f}}\,\cos(\Delta M_{\mathrm{B}^0} t) + S_{\bar{f}}\,\sin(\Delta M_{\mathrm{B}^0} t)\}\,, \qquad (76)$$

where the tiny $\Delta\Gamma_{\mathrm{B}^0}$ corrections have been neglected and we have introduced the notation

$$A_f \equiv A[\mathrm{B}^0 \to f], \qquad \bar{A}_f \equiv -A[\bar{\mathrm{B}}^0 \to f], \qquad \bar{\rho}_f \equiv \bar{A}_f/A_f,$$
$$A_{\bar{f}} \equiv A[\mathrm{B}^0 \to \bar{f}], \qquad \bar{A}_{\bar{f}} \equiv -A[\bar{\mathrm{B}}^0 \to \bar{f}], \qquad \rho_{\bar{f}} \equiv A_{\bar{f}}/\bar{A}_{\bar{f}}, \qquad (77)$$
$$C_f \equiv \frac{1 - |\bar{\rho}_f|^2}{1 + |\bar{\rho}_f|^2}, \qquad S_f \equiv \frac{2\,\mathrm{Im}((q/p)\bar{\rho}_f)}{1 + |\bar{\rho}_f|^2}, \qquad C_{\bar{f}} \equiv -\frac{1 - |\rho_{\bar{f}}|^2}{1 + |\rho_{\bar{f}}|^2}, \qquad S_{\bar{f}} \equiv \frac{-2\,\mathrm{Im}((p/q)\rho_{\bar{f}})}{1 + |\rho_{\bar{f}}|^2}.$$

CP invariance demands that the probabilities of CP-conjugate processes are identical. Thus, CP conservation requires $A_f = \bar{A}_{\bar{f}}$, $A_{\bar{f}} = \bar{A}_f$, $\bar{\rho}_f = \rho_{\bar{f}}$ and $\mathrm{Im}((q/p)\bar{\rho}_f) = \mathrm{Im}((p/q)\rho_{\bar{f}})$, i.e. $C_f = -C_{\bar{f}}$ and $S_f = -S_{\bar{f}}$. Violation of any of the first three equalities would be a signal of direct CP-violation. The fourth equality tests CP-violation generated by the interference of the direct decay $\mathrm{B}^0 \to f$ and the mixing-induced decay $\mathrm{B}^0 \to \bar{\mathrm{B}}^0 \to f$.

For B^0 mesons

$$\left.\frac{q}{p}\right|_{\mathrm{B}^0_{\mathrm{q}}} \;\approx\; \sqrt{\frac{M_{12}^*}{M_{12}}} \;\approx\; \frac{\mathbf{V}_{\mathrm{tb}}^*\mathbf{V}_{\mathrm{tq}}}{\mathbf{V}_{\mathrm{tb}}\mathbf{V}_{\mathrm{tq}}^*} \;\equiv\; \mathrm{e}^{-2\mathrm{i}\varphi_{\mathrm{q}}^M}\,, \qquad (78)$$

where $\varphi_{\mathrm{d}}^M = \beta + \mathcal{O}(\lambda^4)$ and $\varphi_{\mathrm{s}}^M = -\beta_{\mathrm{s}} + \mathcal{O}(\lambda^6)$. The angle β is defined in Eq. (64), while $\beta_{\mathrm{s}} \equiv \arg\left[-(\mathbf{V}_{\mathrm{ts}}\mathbf{V}_{\mathrm{tb}}^*)/(\mathbf{V}_{\mathrm{cs}}\mathbf{V}_{\mathrm{cb}}^*)\right] = \lambda^2\eta + \mathcal{O}(\lambda^4)$ is the equivalent angle in the $\mathrm{B}^0_{\mathrm{s}}$ unitarity triangle, which is predicted to be tiny. Therefore, the mixing ratio q/p is given by a known weak phase.

An obvious example of final states f that can be reached from both the B^0 and the $\bar{\mathrm{B}}^0$ are CP eigenstates; i.e. states such that $\bar{f} = \zeta_f f$ ($\zeta_f = \pm 1$). In this case, $A_{\bar{f}} = \zeta_f A_f$, $\bar{A}_{\bar{f}} = \zeta_f \bar{A}_f$, $\rho_{\bar{f}} = 1/\bar{\rho}_f$, $C_{\bar{f}} = C_f$ and $S_{\bar{f}} = S_f$. A non-zero value of C_f or S_f then signals CP-violation. The ratios $\bar{\rho}_f$ and $\rho_{\bar{f}}$ depend in general on the underlying strong dynamics. However, for CP self-conjugate final states, all dependence on the strong interaction disappears if only one weak amplitude contributes to the $\mathrm{B}^0 \to f$ and $\bar{\mathrm{B}}^0 \to f$ transitions [122, 123]. In this case, we can write the decay amplitude as $A_f = M\mathrm{e}^{\mathrm{i}\varphi^D}\mathrm{e}^{\mathrm{i}\delta_s}$, with $M = M^*$ and φ^D and δ_s weak and strong phases. The ratios $\bar{\rho}_f$ and $\rho_{\bar{f}}$ are then given by

$$\rho_{\bar{f}} \;=\; \bar{\rho}_f^* \;=\; \zeta_f\, e^{2i\varphi^D}\,. \qquad (79)$$

The modulus M and the unwanted strong phase cancel out completely from these two ratios; $\rho_{\bar{f}}$ and $\bar{\rho}_f$ simplify to a single weak phase, associated with the underlying weak quark transition. Since $|\rho_{\bar{f}}| = |\bar{\rho}_f| = 1$, the time-dependent decay probabilities become much simpler. In particular, $C_f = 0$ and there is no longer any dependence on $\cos(\Delta M_{\mathrm{B}^0} t)$. Moreover, the coefficients of the sinusoidal terms are then fully known in terms of CKM mixing angles only: $S_f = S_{\bar{f}} = -\zeta_f \sin[2(\varphi_{\mathrm{q}}^M + \varphi^D)] \equiv -\zeta_f \sin(2\Phi)$. In this ideal case, the time-dependent CP-violating decay asymmetry

$$\frac{\Gamma[\bar{\mathrm{B}}^0(t) \to \bar{f}] - \Gamma[\mathrm{B}^0(t) \to f]}{\Gamma[\bar{\mathrm{B}}^0(t) \to \bar{f}] + \Gamma[\mathrm{B}^0(t) \to f]} \;=\; -\zeta_f \sin(2\Phi)\,\sin(\Delta M_{\mathrm{B}^0} t) \qquad (80)$$

provides a direct and clean measurement of the CKM parameters [124].

When several decay amplitudes with different phases contribute, $|\bar{\rho}_f| \neq 1$ and the interference term will depend both on CKM parameters and on the strong dynamics embodied in $\bar{\rho}_f$. The leading contributions to $\bar{\mathrm{b}} \to \bar{\mathrm{q}}'\mathrm{q}'\bar{\mathrm{q}}$ are either the tree-level W exchange or penguin topologies generated by gluon

Table 3: CKM factors and relevant angle Φ for some B decays into CP eigenstates.

Decay	Tree-level CKM	Penguin CKM	Exclusive channels	Φ
$\bar{b} \to \bar{c}c\bar{s}$	$A\lambda^2$	$-A\lambda^2$	$B_d^0 \to J/\psi K_S, J/\psi K_L$	β
			$B_s^0 \to D_s^+ D_s^-, J/\psi\phi$	$-\beta_s$
$\bar{b} \to \bar{s}s\bar{s}$		$-A\lambda^2$	$B_d^0 \to K_S\phi, K_L\phi$	β
			$B_s^0 \to \phi\phi$	$-\beta_s$
$\bar{b} \to \bar{d}d\bar{s}$		$-A\lambda^2$	$B_s^0 \to K_S K_S, K_L K_L$	$-\beta_s$
$\bar{b} \to \bar{c}c\bar{d}$	$-A\lambda^3$	$A\lambda^3(1-\rho-\mathrm{i}\eta)$	$B_d^0 \to D^+D^-, J/\psi\pi^0$	$\approx \beta$
			$B_s^0 \to J/\psi K_S, J/\psi K_L$	$\approx -\beta_s$
$\bar{b} \to \bar{u}u\bar{d}$	$A\lambda^3(\rho+\mathrm{i}\eta)$	$A\lambda^3(1-\rho-\mathrm{i}\eta)$	$B_d^0 \to \pi^+\pi^-, \rho^0\pi^0, \omega\pi^0$	$\approx \beta+\gamma$
			$B_s^0 \to \rho^0 K_{S,L}, \omega K_{S,L}, \pi^0 K_{S,L}$	$\neq \gamma-\beta_s$
$\bar{b} \to \bar{s}s\bar{d}$		$A\lambda^3(1-\rho-\mathrm{i}\eta)$	$B_d^0 \to K_S K_S, K_L K_L, \phi\pi^0$	0
			$B_s^0 \to K_S\phi, K_L\phi$	$-\beta-\beta_s$

(γ, Z) exchange. Although of higher order in the strong (electroweak) coupling, penguin amplitudes are logarithmically enhanced by the virtual W loop and are potentially competitive. Table 3 contains the CKM factors associated with the two topologies for different B decay modes into CP eigenstates.

The gold-plated decay mode is $B_d^0 \to J/\psi K_S$. In addition to having a clean experimental signature, the two topologies have the same (zero) weak phase. The CP asymmetry then provides a clean measurement of the mixing angle β, without strong-interaction uncertainties. Fig. 7 shows the most recent BELLE measurement [125] of time-dependent $\bar{b} \to c\bar{c}\bar{s}$ asymmetries for CP-odd ($B_d^0 \to J/\psi K_S$, $B_d^0 \to \psi' K_S$, $B_d^0 \to \chi_{c1} K_S$) and CP-even ($B_d^0 \to J/\psi K_L$) final states. A very nice oscillation is manifest, with opposite signs for the two different choices of $\zeta_f = \pm 1$. Including the information obtained from other $\bar{b} \to c\bar{c}\bar{s}$ decays, one gets the world average [57]

$$\sin(2\beta) = 0.68 \pm 0.02. \tag{81}$$

Fitting an additional $\cos(\Delta M_{B^0} t)$ term in the measured asymmetries results in $C_f = 0.013 \pm 0.017$ [57], confirming the expected null result. An independent measurement of $\sin 2\beta$ can be obtained from $\bar{b} \to s\bar{s}\bar{s}$ and $\bar{b} \to d\bar{d}\bar{s}$ decays, which only receive penguin contributions and, therefore, could be more sensitive to new-physics corrections in the loop diagram. These modes give $\sin(2\beta) = 0.64 \pm 0.04$ [57], in perfect agreement with (81).

Eq. (81) determines the angle β up to a four-fold ambiguity. The time-dependent analysis of the angular $B_d^0 \to J/\psi K^{*0}$ distribution and the Dalitz plot of $B_d^0 \to \bar{D}_0 h^0$ decays ($h^0 = \pi^0, \eta, \omega$) allows us to resolve the $\beta \longleftrightarrow \frac{1}{2}\pi - \beta$ ambiguity (but not the $\beta \longleftrightarrow \pi + \beta$), showing that negative $\cos(2\beta)$ solutions are very unlikely [126,127]. The result fits nicely with all previous unitarity triangle constraints in Fig. 5.

A determination of $\beta + \gamma = \pi - \alpha$ can be obtained from $\bar{b} \to \bar{u}u\bar{d}$ decays, such as $B_d^0 \to \pi\pi$ or $B_d^0 \to \rho\rho$. However, the penguin contamination, which carries a different weak phase, can be sizeable. The time-dependent asymmetry in $B_d^0 \to \pi^+\pi^-$ shows indeed a non-zero value for the $\cos(\Delta M_{B^0} t)$ term, $C_f = -0.38 \pm 0.06$ [57], indicating the presence of an additional amplitude; then $S_f = -0.65 \pm 0.07 \neq \sin 2\alpha$. One could still extract useful information on α (up to 16 mirror solutions), using the isospin relations among the $B_d^0 \to \pi^+\pi^-$, $B_d^0 \to \pi^0\pi^0$ and $B^+ \to \pi^+\pi^0$ amplitudes and their CP conjugates [128]; however, only a loose constraint is obtained given the limited experimental precision on $B_d^0 \to \pi^0\pi^0$. Much stronger constraints are obtained from $B_d^0 \to \rho\rho$ because one can use the additional polarization information of two vectors in the final state to resolve the different contributions.

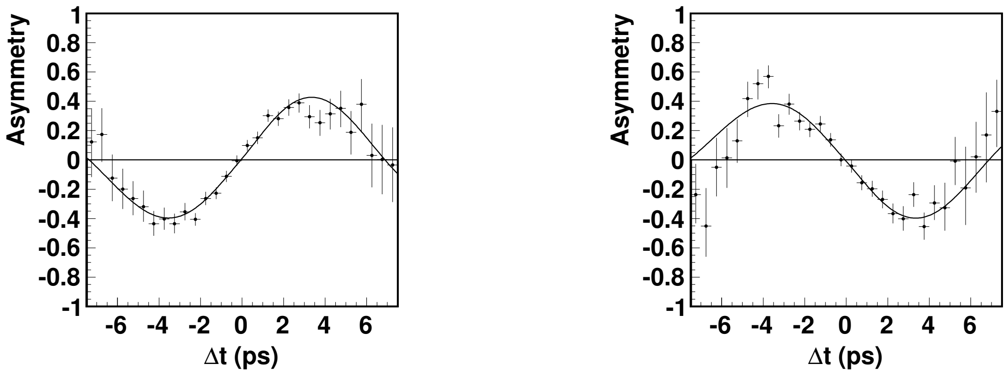

Fig. 7: Time-dependent asymmetries for (left) CP-odd ($\mathrm{B_d^0} \to \mathrm{J}/\psi \mathrm{K}_S$, $\mathrm{B_d^0} \to \psi' \mathrm{K}_S$, $\mathrm{B_d^0} \to \chi_{c1} \mathrm{K}_S$; $\zeta_f = -1$) and (right) CP-even ($\mathrm{B_d^0} \to \mathrm{J}/\psi \mathrm{K}_L$; $\zeta_f = +1$) final states, measured by BELLE [125].

Moreover, the small branching fraction $\mathrm{Br}(\mathrm{B_d^0} \to \rho^0\rho^0) = (0.73\,^{+\,0.27}_{-\,0.28}) \times 10^{-6}$ [13] implies a very small penguin contribution. Additional information can be obtained from $\mathrm{B_d^0}, \bar{\mathrm{B}}_\mathrm{d}^0 \to \rho^\pm\pi^\mp$, although the final states are not CP eigenstates. Combining all pieces of information results in [13, 104]

$$\alpha \,=\, (89.0\,^{+\,4.4}_{-\,4.2})^\circ \,. \tag{82}$$

The angle γ cannot be determined in $\bar{\mathrm{b}} \to \mathrm{u\bar{u}\bar{d}}$ decays such as $\mathrm{B_s^0} \to \rho^0 \mathrm{K}_S$ because the colour factors in the hadronic matrix element enhance the penguin amplitude with respect to the tree-level contribution. Instead, γ can be measured through the tree-level decays $\mathrm{B}^- \to \mathrm{D_0 K^-}$ ($\mathrm{b} \to \mathrm{c\bar{u}s}$) and $\mathrm{B}^- \to \bar{\mathrm{D}}_0 \mathrm{K}^-$ ($\mathrm{b} \to \mathrm{u\bar{c}s}$), using final states accessible in both D_0 and $\bar{\mathrm{D}}_0$ decays and playing with the interference of both amplitudes [129–131]. The sensitivity can be optimized with Dalitz-plot analyses of $\mathrm{D}_0, \bar{\mathrm{D}}_0 \to \mathrm{K}_S\pi^+\pi^-$ decays. The extensive studies made by BABAR and BELLE result in [13, 104]

$$\gamma \,=\, (73\,^{+\,22}_{-\,25})^\circ \,. \tag{83}$$

Mixing-induced CP-violation has also been sought in the decays $\mathrm{B_s^0} \to \mathrm{J}/\psi\phi$ and $\mathrm{B_s^0} \to \mathrm{J}/\psi f_0(980)$. From the corresponding time-dependent CP asymmetries, LHCb has recently determined the angle [119]

$$\beta_s \,=\, -(2 \pm 5)^\circ \,, \tag{84}$$

in good agrement with the SM prediction $\beta_s \approx \eta\lambda^2 \approx 1^\circ$.

6.3 Global fit of the unitarity triangle

The CKM parameters can be more accurately determined through a global fit to all available measurements, imposing the unitarity constraints and taking properly into account the theoretical uncertainties. The global fit shown in Fig. 5 uses frequentist statistics and gives [104]

$$\lambda \,=\, 0.2254\,^{+\,0.0006}_{-\,0.0010} \,, \qquad A \,=\, 0.801\,^{+\,0.026}_{-\,0.014} \,, \qquad \bar{\rho} \,=\, 0.144\,^{+\,0.023}_{-\,0.026} \,, \qquad \bar{\eta} \,=\, 0.343\,^{+\,0.015}_{-\,0.014} \,. \tag{85}$$

This implies $\mathcal{J} = (2.884\,^{+\,0.253}_{-\,0.053}) \times 10^{-5}$, $\alpha = (90.9\,^{+\,3.5}_{-\,4.1})^\circ$, $\beta = (21.84\,^{+\,0.80}_{-\,0.76})^\circ$ and $\gamma = (67.3\,^{+\,4.2}_{-\,3.5})^\circ$. Similar results are obtained by the UTfit group [132], using instead a Bayesian approach and a slightly different treatment of theoretical uncertainties.

6.4 Direct CP-violation in B and D decays

The B factories have established the presence of direct CP-violation in several decays of B mesons. The most significant signals are [13, 57]

$$\mathcal{A}^{\mathrm{CP}}_{\bar{\mathrm{B}}^0_\mathrm{d} \to \mathrm{K}^-\pi^+} = -0.098 \pm 0.013, \qquad \mathcal{A}^{\mathrm{CP}}_{\bar{\mathrm{B}}^0_\mathrm{d} \to \bar{\mathrm{K}}^{*0}\eta} = 0.19 \pm 0.05, \qquad \mathcal{A}^{\mathrm{CP}}_{\bar{\mathrm{B}}^0_\mathrm{d} \to \mathrm{K}^{*-}\pi^+} = -0.19 \pm 0.07,$$

$$C_{\mathrm{B_d^0}\to\pi^+\pi^-} = -0.38 \pm 0.06\,, \qquad \mathcal{A}^{\mathrm{CP}}_{\mathrm{B^-\to K^- D_{CP(+1)}}} = 0.24 \pm 0.06\,,$$
$$\mathcal{A}^{\mathrm{CP}}_{\mathrm{B^-\to K^-}\rho^0} = 0.37 \pm 0.10\,, \qquad \mathcal{A}^{\mathrm{CP}}_{\mathrm{B^-\to K^-}\eta} = -0.37 \pm 0.09\,,$$
$$\mathcal{A}^{\mathrm{CP}}_{\mathrm{B^-\to K^-} f_2(1270)} = -0.68\,^{+\,0.19}_{-\,0.17}\,, \qquad \mathcal{A}^{\mathrm{CP}}_{\mathrm{B^-}\to\pi^- f_0(1370)} = 0.72 \pm 0.22\,. \tag{86}$$

LHCb has also reported evidence for direct CP-violation in D decays [133]:

$$\mathcal{A}^{\mathrm{CP}}_{\mathrm{D_0\to K^+K^-}} - \mathcal{A}^{\mathrm{CP}}_{\mathrm{D_0}\to\pi^+\pi^-} = -0.82 \pm 0.24\,. \tag{87}$$

Unfortunately, owing to the unavoidable presence of strong phases, a real theoretical understanding of the corresponding SM predictions is still lacking. Progress in this direction is needed to perform meaningful tests of the CKM mechanism of CP-violation and to pin down any possible effects from new physics beyond the SM framework.

7 Rare decays

Complementary and very valuable information could also be obtained from rare decays, which in the SM are strongly suppressed by the GIM mechanism. These processes are sensitive to new-physics contributions with a different flavour structure. Well-known examples are the kaon decay modes $\mathrm{K}^\pm \to \pi^\pm\nu\bar{\nu}$ and $\mathrm{K}_L \to \pi^0\nu\bar{\nu}$, where long-distance effects play a negligible role. The decay amplitudes are dominated by short-distance loops (Z penguin, W box) involving the heavy top quark, but receive also sizeable contributions from internal charm exchanges. The relevant hadronic matrix elements can be obtained from $\mathrm{K}_{\ell 3}$ decays, assuming isospin symmetry. The neutral decay is CP-violating and proceeds almost entirely through direct CP-violation (via interference with mixing). Taking the CKM matrix elements from the global fit, the predicted SM rates are [134–136]:

$$\mathrm{Br}(\mathrm{K}^+ \to \pi^+\nu\bar{\nu})^{\mathrm{th}} = (0.78 \pm 0.08) \times 10^{-10}\,, \qquad \mathrm{Br}(\mathrm{K}_L \to \pi^0\nu\bar{\nu})^{\mathrm{th}} = (2.4 \pm 0.4) \times 10^{-11}\,. \tag{88}$$

On the experimental side, the charged kaon mode was already observed [137], while only an upper bound on the neutral mode has been achieved [138]:

$$\mathrm{Br}(\mathrm{K}^+ \to \pi^+\nu\bar{\nu}) = (1.73^{+1.15}_{-1.05}) \times 10^{-10}\,, \qquad \mathrm{Br}(\mathrm{K}_L \to \pi^0\nu\bar{\nu}) < 2.6 \times 10^{-8} \quad (90\%\ \mathrm{CL}). \tag{89}$$

New experiments are under development at CERN [139] and J-PARC [140] for charged and neutral modes, respectively, aiming to reach $\mathcal{O}(100)$ events and begin to seriously probe the new-physics potential of these decays. Increased sensitivities could be obtained through the recent P996 proposal for a $\mathrm{K}^+ \to \pi^+\nu\bar{\nu}$ experiment at Fermilab and the higher kaon fluxes available at Project-X [141].

Another promising mode is $\mathrm{K}_L \to \pi^0\mathrm{e}^+\mathrm{e}^-$. Owing to the electromagnetic suppression of the 2γ CP-conserving contribution, this decay is dominated by the CP-violating one-photon emission amplitude. It receives contributions from both direct and indirect CP-violation, which amount to a predicted rate $\mathrm{Br}(\mathrm{K}_L \to \pi^0\mathrm{e}^+\mathrm{e}^-)^{\mathrm{th}} = (3.1 \pm 0.9) \times 10^{-11}$ [44], 10 times smaller than the present experimental bound $\mathrm{Br}(\mathrm{K}_L \to \pi^0\mathrm{e}^+\mathrm{e}^-) < 2.8 \times 10^{-10}$ (90% CL) [142]. Other interesting K decays are discussed in [44].

The inclusive decay $\bar{\mathrm{B}} \to \mathrm{X}_s\gamma$ provides another powerful test of the SM flavour structure at the quantum loop level. The present experimental world average [57] $\mathrm{Br}(\bar{\mathrm{B}} \to \mathrm{X}_s\gamma)_{E_\gamma \geq 1.6\ \mathrm{GeV}} = (3.55 \pm 0.26) \times 10^{-4}$ agrees very well with the SM theoretical prediction [143] at the next-to-next-to-leading-order (NNLO), $\mathrm{Br}(\bar{\mathrm{B}} \to \mathrm{X}_s\gamma)^{\mathrm{th}}_{E_\gamma \geq 1.6\ \mathrm{GeV}} = (3.15 \pm 0.23) \times 10^{-4}$. Other interesting processes with B mesons are $\bar{\mathrm{B}} \to \mathrm{K}^{(*)}\ell^+\ell^-$, $\bar{\mathrm{B}}^0 \to \ell^+\ell^-$ and $\bar{\mathrm{B}} \to \mathrm{K}^{(*)}\nu\bar{\nu}$ [34].

8 Discussion

The flavour structure of the SM is one of the main questions still remaining in our understanding of weak interactions. Although we do not know the reason for the observed family replication, we have learnt experimentally that the number of SM generations is just three (and no more). Therefore, we must study as precisely as possible the few existing flavours, to get some hints on the dynamics responsible for their observed structure.

In the SM, all flavour dynamics originate in the fermion mass matrices, which determine the measurable masses and mixings. The SM incorporates a mechanism to generate CP-violation, through the single phase naturally occurring in the CKM matrix. This mechanism, deeply rooted in the unitarity structure of $\mathbf{V}$, implies very specific requirements for CP-violation to show up. The CKM matrix has been thoroughly investigated in dedicated experiments, and a large number of CP-violating processes have been studied in detail. At present, all flavour data seem to fit into the SM framework, confirming that the fermion mass matrices are the dominant source of flavour-mixing phenomena. However, a fundamental explanation of the flavour dynamics is still lacking.

The dynamics of flavour is a broad and fascinating subject, which is closely related to the as-yet untested scalar sector of the SM. LHC has already excluded a broad range of Higgs masses, narrowing down the SM Higgs hunt to the region of low masses between 115.5 and 127 GeV (95% CL) [144, 145]. This is precisely the range of masses preferred by precision electroweak tests [4]. The discovery of a neutral scalar boson in this mass range would provide a spectacular confirmation of the SM framework.

If the Higgs boson does not show up soon, we should look for alternative mechanisms of mass generation, satisfying the many experimental constraints that the SM has successfully fulfilled so far. The easiest perturbative way would be to enlarge the scalar sector with additional Higgs doublets, without spoiling the electroweak precision tests. However, adding more scalar doublets to the Yukawa Lagrangian (4) leads to new sources of flavour-changing phenomena; in particular, the additional neutral scalars acquire tree-level flavour-changing neutral couplings, which represent a major phenomenological problem. In order to satisfy the stringent experimental constraints, these scalars should be either decoupled (very large masses above 10–50 TeV or tiny couplings) or have their Yukawa couplings aligned in flavour space [146], which suggests the existence of additional flavour symmetries at higher scales. The usual supersymmetric models with two scalar doublets avoid this problem through a discrete symmetry, which only allows one of the scalars to couple to a given right-handed fermion [147]. However, the presence of flavoured supersymmetric partners gives rise to other problematic sources of flavour and CP phenomena, making it necessary to tune their couplings to be tiny (or zero) [148]. Models with dynamical electroweak symmetry breaking also have difficulties in accommodating the flavour constraints in a natural way. Thus, flavour phenomena impose severe restrictions on possible extensions of the SM.

New experimental input is expected from LHCb, BESS-III, the future Super-Belle and Super-B factories and from several kaon (NA62, DAΦNE, $\mathrm{K_0}$TO, TREK, KLOD, OKA, Project-X) and muon (MEG, Mu2e, COMET, PRISM) experiments. These data will provide very valuable information, complementing the high-energy searches for new phenomena at LHC. Unexpected surprises may well be discovered, probably giving hints of new physics at higher scales and offering clues to the problems of fermion mass generation, quark mixing and family replication.

Acknowledgements

I want to thank the organizers for the charming atmosphere of this School and all the students for their many interesting questions and comments. I am also grateful for the hospitality of the Physics Department of the Technical University of Munich, where these lectures were written, and for the support of the Alexander von Humboldt Foundation. This work has been supported in part by MICINN, Spain (FPA2007-60323 and Consolider-Ingenio 2010 Program CSD2007-00042 – CPAN) and Generalitat Valenciana (Prometeo/2008/069).

References

[1] S.L. Glashow, *Nucl. Phys.* **22** (1961) 579.

[2] S. Weinberg, *Phys. Rev. Lett.* **19** (1967) 1264.

[3] A. Salam, in *Elementary Particle Theory*, Ed. N. Svartholm (Almquist and Wiksells, Stockholm, 1969), p. 367.

[4] A. Pich, in The Standard Model of electroweak interactions, Reports CERN-2006-003 and CERN-2007-005, Ed. R. Fleischer, p. 1 [arXiv:hep-ph/0502010, arXiv:0705.4264 [hep-ph]].

[5] N. Cabibbo, *Phys. Rev. Lett.* **10** (1963) 531.

[6] M. Kobayashi and T. Maskawa, *Prog. Theor. Phys.* **42** (1973) 652.

[7] S.L. Glashow, J. Iliopoulos and L. Maiani, *Phys. Rev.* **D2** (1970) 1285.

[8] MEG Collaboration, *Phys. Rev. Lett.* **107** (2011) 171801.

[9] SINDRUM Collaboration, *Nucl. Phys.* **B299** (1988) 1.

[10] R.D. Bolton *et al.*, *Phys. Rev.* **D38** (1988) 2077.

[11] BABAR Collaboration, *Phys. Rev. Lett.* **95** (2005) 191801; ibid. **98** (2007) 061803; ibid. **99** (2007) 251803; ibid. **100** (2008) 071802; ibid. **103** (2009) 021801; ibid. **104** (2010) 021802; *Phys. Rev.* **D79** (2009) 012004; ibid. **D81** (2010) 111101.

[12] BELLE Collaboration, *Phys. Lett.* **B648** (2007) 341; ibid. **B660** (2008) 154; ibid. **B664** (2008) 35; ibid. **B666** (2008) 16; ibid. **B672** (2009) 317; ibid. **B682** (2010) 355; ibid. **B687** (2010) 139; ibid. **B692** (2010) 4.

[13] K. Nakamura *et al.*, *J. Phys.* **G37** (2010) 075021.

[14] W.J. Marciano and A. Sirlin, *Phys. Rev. Lett.* **61** (1988) 1815.

[15] T. van Ritbergen and R.G. Stuart, *Phys. Rev. Lett.* **82** (1999) 488; *Nucl. Phys.* **B564** (2000) 343.

[16] A. Pak and A. Czarnecki, *Phys. Rev. Lett.* **100** (2008) 241807.

[17] MuLan Collaboration, *Phys. Rev. Lett* **106** (2011) 041803.

[18] E. Braaten, S. Narison and A. Pich, *Nucl. Phys.* **B373** (1992) 581.

[19] A. Pich, "Tau Decay Determination of the QCD Coupling," arXiv:1107.1123.

[20] BABAR Collaboration, *Phys. Rev. Lett.* **105** (2010) 051602.

[21] NA62 Collaboration, *Phys. Lett.* **B698** (2011) 105.

[22] Flavianet Kaon Working Group, *Eur. Phys. J.* **C69** (2010) 399.

[23] A. Pich, "Flavordynamics", arXiv:hep-ph/9601202.

[24] W.J. Marciano and A. Sirlin, *Phys. Rev. Lett.* **96** (2006) 032002; ibid. **71** (1993) 3629.

[25] A. Czarnecki, W.J. Marciano and A. Sirlin, *Phys. Rev.* **D70** (2004) 093006.

[26] J.C. Hardy and I.S. Towner, *Phys. Rev.* **C79** (2009) 055502; ibid. **C77** (2008) 025501; *Rep. Prog. Phys.* **73** (2010) 046301.

[27] A. Serebrov *et al.*, *Phys. Lett.* **B605** (2005) 72.

[28] A. Pichlmaier *et al.*, *Phys. Lett.* **B693** (2010) 221.

[29] J.S. Nico *et al.*, *Phys. Rev.* **C71** (2005) 055502.

[30] H. Abele, *Prog. Part. Nucl. Phys.* **60** (2008) 1.

[31] M. Ademollo and R. Gatto, *Phys. Rev. Lett.* **13** (1964) 264.

[32] V. Cirigliano, M. Knecht, H. Neufeld and H. Pichl, *Eur. Phys. J.* **C27** (2003) 255.

[33] D. Pocanic *et al.*, *Phys. Rev. Lett.* **93** (2004) 181803.

[34] M. Antonelli *et al.*, *Phys. Rep.* **494** (2010) 197.

[35] V. Cirigliano, M. Giannotti and H. Neufeld, *J. High Energy Phys.* **0811** (2008) 006.

[36] A. Kastner and H. Neufeld, *Eur. Phys. J.* **C57** (2008) 541.

[37] R.E. Behrends and A. Sirlin, *Phys. Rev. Lett.* **4** (1960) 186.
[38] H. Leutwyler and M. Roos, *Z. Phys.* **C25** (1984) 91.
[39] M. Jamin, J.A. Oller and A. Pich, *J. High Energy Phys.* **0402** (2004) 047.
[40] V. Cirigliano *et al.*, *J. High Energy Phys.* **0504** (2005) 006.
[41] J. Bijnens and P. Talavera, *Nucl. Phys.* **B669** (2003) 341.
[42] G. Colangelo *et al.*, *Eur. Phys. J.* **C71** (2011) 1695.
[43] RBC-UKQCD Collaboration, *Eur. Phys. J.* **C69** (2010) 159.
[44] V. Cirigliano, G. Ecker, H. Neufeld, A. Pich and J. Portolés, *Rev. Mod. Phys.* **84** (2012) 399.
[45] W.J. Marciano, *Phys. Rev. Lett.* **93** (2004) 231803.
[46] V. Cirigliano and H. Neufeld, *Phys. Lett.* **B700** (2011) 7.
[47] N. Cabibbo, E.C. Swallow and R. Winston, *Annu. Rev. Nucl. Part. Sci.* **53** (2003) 39; *Phys. Rev. Lett.* **92** (2004) 251803.
[48] V. Mateu and A. Pich, *J. High Energy Phys.* **0510** (2005) 041.
[49] E. Gámiz, M. Jamin, A. Pich, J. Prades and F. Schwab, *Phys. Rev. Lett.* **94** (2005) 011803; *J. High Energy Phys.* **0301** (2003) 060.
[50] A. Pich, *Nucl. Phys. (Proc. Suppl.)* **218** (2011) 89.
[51] N. Isgur and M. Wise, *Phys. Lett.* **B232** (1989) 113; ibid. **B237** (1990) 527.
[52] B. Grinstein, *Nucl. Phys.* **B339** (1990) 253.
[53] E. Eichten and B. Hill, *Phys. Lett.* **B234** (1990) 511.
[54] H. Georgi, *Phys. Lett.* **B240** (1990) 447.
[55] M. Neubert, *Phys. Lett.* **B264** (1991) 455.
[56] M. Luke, *Phys. Lett.* **B252** (1990) 447.
[57] Heavy Flavour Averaging Group, arXiv:1010.1589 [hep-ex]. http://www.slac.stanford.edu/xorg/hfag.
[58] C. Bernard *et al.*, *Phys. Rev.* **D79** (2009) 014506; *Proc. Sci.* PoS (Lattice 2010) 311.
[59] M. Okamoto, *Proc. Sci.* PoS (LAT2005) 013.
[60] P. Gambino, T. Mannel and N. Uraltsev, *Phys. Rev.* **D81** (2010) 113002.
[61] I.I.Y. Bigi *et al.*, *Phys. Rev. Lett.* **71** (1993) 496; *Phys. Lett.* **B323** (1994) 408.
[62] A.V. Manohar and M.B. Wise, *Phys. Rev.* **D49** (1994) 1310.
[63] D. Benson, I.I. Bigi, T. Mannel and N. Uraltsev, *Nucl. Phys.* **B665** (2003) 367.
[64] P. Gambino and N. Uraltsev, *Eur. Phys. J.* **C34** (2004) 181.
[65] D. Benson, I.I. Bigi and N. Uraltsev, *Nucl. Phys.* **B710** (2005) 371.
[66] O. Buchmuller and H. Flacher, *Phys. Rev.* **D73** (2006) 073008.
[67] C.W. Bauer, Z. Ligeti, M. Luke, A.V. Manohar and M. Trott, *Phys. Rev.* **D70** (2004) 094017.
[68] P. Gambino, *J. High Energy Phys.* **1109** (2011) 055.
[69] P. Ball and R. Zwicky, *Phys. Rev.* **D71** (2005) 014015.
[70] G. Duplancic *et al.*, *J. High Energy Phys.* **0804** (2008) 014.
[71] A. Khodjamirian *et al.*, *Phys. Rev.* **D83** (2011) 094031.
[72] E. Dalgic *et al.*, *Phys. Rev.* **D73** (2006) 074502 [Erratum, ibid. **D75** (2007) 119906].
[73] J.A. Bailey *et al.*, *Phys. Rev.* **D79** (2009) 054507.
[74] B.O. Lange *et al.*, *Phys. Rev.* **D72** (2005) 073006; *Nucl. Phys.* **B699** (2004) 335.
[75] J.R. Andersen and E. Gardi, *J. High Energy Phys.* **0601** (2006) 097.
[76] P. Gambino, P. Giordano, G. Ossola and N. Uraltsev, *J. High Energy Phys.* **0710** (2007) 058.
[77] U. Aglietti, F. Di Lodovico, G. Ferrera and G. Ricciardi, *Eur. Phys. J.* **C59** (2009) 831.

[78] C. Greub, M. Neubert and B.D. Pecjak, *Eur. Phys. J.* **C65** (2010) 501.
[79] G. Paz, *J. High Energy Phys.* **0906** (2009) 083.
[80] Z. Ligeti *et al.*, *Phys. Rev.* **D82** (2010) 033003; ibid. **D78** (2008) 114014; arXiv:1101.3310 [hep-ph].
[81] P. Gambino and J.F. Kamenik, *Nucl. Phys.* **B840** (2010) 424.
[82] H. Na *et al.*, *Phys. Rev.* **D82** (2010) 114506.
[83] C. Bernard *et al.*, *Phys. Rev.* **D80** (2009) 034026; *Phys. Rev. Lett.* **94** (2005) 011601.
[84] CLEO Collaboration, *Phys. Rev.* **D80** (2009) 032005.
[85] J. Lahio, B.D. Pecjak and C. Schwanda, arXiv:1107.3934.
[86] D0 Collaboration, *Phys. Rev. Lett.* **100** (2008) 192003.
[87] CDF Collaboration, *Phys. Rev. Lett.* **95** (2005) 102002.
[88] D0 Collaboration, *Phys. Rev. Lett.* **103** (2009) 092001.
[89] CDF Collaboration, *Phys. Rev. Lett.* **103** (2009) 092002; *Phys. Rev.* **D81** (2010) 072003.
[90] ALEPH, CDF, D0, DELPHI, L3, OPAL and SLD Collaborations, LEP Electroweak Working Group, Tevatron Electroweak Working Group and SLD Electroweak and Heavy Flavour Groups, arXiv:1012.2367 [hep-ex]; http://www.cern.ch/LEPEWWG/.
[91] ALEPH, DELPHI, L3, OPAL and SLD Collaborations, LEP Electroweak Working Group and SLD Electroweak and Heavy Flavour Groups, *Phys. Rep.* **427** (2006) 257.
[92] L. Wolfenstein, *Phys. Rev. Lett.* **51** (1983) 1945.
[93] A.J. Buras, M.E. Lautenbacher and G. Ostermaier, *Phys. Rev.* **D50** (1994) 3433.
[94] T. Inami and C.S. Lim, *Progr. Theor. Phys.* **65** (1981) 297.
[95] M.K. Gaillard and B.W. Lee, *Phys. Rev.* **D10** (1974) 897.
[96] ARGUS Collaboration, *Phys. Lett.* **B192** (1987) 245.
[97] CDF Collaboration, *Phys. Rev. Lett.* **97** (2006) 242003.
[98] LHCb Collaboration, LHCb-CONF-2011-050 (2011).
[99] A.J. Buras, M. Jamin and P.H. Weisz, *Nucl. Phys.* **B347** (1990) 491.
[100] S. Herrlich and U. Nierste, *Nucl. Phys.* **B419** (1994) 292; **B476** (1996) 27.
[101] A. Pich and J. Prades, *Phys. Lett.* **B346** (1995) 342.
[102] E. Gámiz *et al.*, *Phys. Rev.* **D80** (2009) 014503.
[103] C. Jarlskog, *Phys. Rev. Lett.* **55** (1985) 1039; *Z. Phys.* **C29** (1985) 491.
[104] CKMfitter Group, *Eur. Phys. J.* **C41** (2005) 1.
[105] NA48 Collaboration, *Phys. Lett.* **B544** (2002) 97; ibid. **B465** (1999) 335; *Eur. Phys. J.* **C22** (2001) 231.
[106] KTeV Collaboration, *Phys. Rev.* **D83** (2011) 092001; ibid. **D67** (2003) 012005; *Phys. Rev. Lett.* **83** (1999) 22.
[107] NA31 Collaboration, *Phys. Lett.* **B317** (1993) 233; ibid. **B206** (1988) 169.
[108] E731 Collaboration, *Phys. Rev. Lett.* **70** (1993) 1203.
[109] A.J. Buras, M. Jamin and M.E. Lautenbacher, *Nucl. Phys.* **B408** (1993) 209; *Phys. Lett.* **B389** (1996) 749.
[110] M. Ciuchini *et al.*, *Phys. Lett.* **B301** (1993) 263; *Z. Phys.* **C68** (1995) 239.
[111] E. Pallante and A. Pich, *Phys. Rev. Lett.* **84** (2000) 2568; *Nucl. Phys.* **B592** 294.
[112] E. Pallante, A. Pich and I. Scimemi, *Nucl. Phys.* **B617** (2001) 441.
[113] V. Cirigliano, A. Pich, G. Ecker and H. Neufeld, *Phys. Rev. Lett.* **91** (2003) 162001.
[114] G. Buchalla, A.J. Buras and M.E. Lautenbacher, *Rev. Mod. Phys.* **68** (1996) 1125.

[115] J. Brod and M. Gorbahn, *Phys. Rev.* **D82** (2010) 094026.

[116] D0 Collaboration, *Phys. Rev.* **D84** (2011) 052007; ibid. **D82** (2010) 032001; *Phys. Rev. Lett.* **105** (2010) 081801.

[117] A. Lenz and U. Nierste, *J. High Energy Phys.* **0706** (2007) 072.

[118] J. Charles *et al.*, *Phys. Rev.* **D84** (2011) 033005.

[119] LHCb Collaboration, arXiv:1112.3183 [hep-ex];
Phys. Lett. **B707** (2012) 497.

[120] CDF Collaboration, *Phys. Rev.* **D85** (2012) 072002.

[121] D0 Collaboration, *Phys. Rev.* **D85** (2012) 032006.

[122] A.B. Carter and A.I. Sanda, *Phys. Rev. Lett.* **45** (1980) 952; *Phys. Rev.* **D23** (1981) 1567.

[123] I.I. Bigi and A.I. Sanda, *Nucl. Phys.* **B193** (1981) 85.

[124] P. Krawczyk *et al.*, *Nucl. Phys.* **B307** (1988) 19.

[125] H.B. Sahoo (for the BELLE Collaboration), arXiv:1109.4780 [hep-ex].

[126] BABAR Collaboration, *Phys. Rev.* **D71** (2005) 032005; *Phys. Rev. Lett.* **99** (2007) 231802.

[127] BELLE Collaboration, *Phys. Rev. Lett.* **95** (2005) 091601; ibid. **97** (2006) 081801.

[128] M. Gronau and D. London, *Phys. Rev. Lett.* **65** (1990) 3381.

[129] M. Gronau and D. London, *Phys. Lett.* **B253** (1991) 483.

[130] M. Gronau and D. Wyler, *Phys. Lett.* **B265** (1991) 172.

[131] D. Atwood *et al.*, *Phys. Rev. Lett* **78** (1997) 3257; *Phys. Rev.* **D63** (2001) 036005.

[132] UTfit Collaboration, *J. High Energy Phys.* **0507** (2005) 028.

[133] LHCb Collaboration, *Phys. Rev. Lett.* **108** (2012) 111602.

[134] J. Brod, M. Gorbahn and E. Stamou, *Phys. Rev.* **D83** (2011) 034030.

[135] A.J. Buras, F. Schwab and S. Uhli, *Rev. Mod. Phys.* **80** (2008) 965.

[136] A.J. Buras *et al.*, *Phys. Rev. Lett.* **95** (2005) 261805; *J. High Energy Phys.* **0611** (2006) 002.

[137] E949 Collaboration, *Phys. Rev. Lett.* **101** (2008) 191802.

[138] E391a Collaboration, *Phys. Rev. Lett.* **100** (2008) 201802; *Phys. Rev.* **D81** (2010) 072004.

[139] T. Spadaro (for the NA62 Collaboration), arXiv:1101.5631 [hep-ex].

[140] H. Watanabe (for the J-PARC E14 KOTO Collaboration), *Proc. Sci.* PoS (ICHEP 2010) 274.

[141] R. Tschirhart, *Nucl. Phys. (Proc. Suppl.)* **210–211** (2011) 220.

[142] KTeV Collaboration *Phys. Rev. Lett.* **93** (2004) 021805.

[143] M. Misiak *et al.*, *Phys. Rev. Lett.* **98** (2007) 022002.

[144] ATLAS Collaboration, ATLAS-CONF-2011-163.

[145] CMS Collaboration, CMS PAS HIG-11-032 (2011).

[146] A. Pich, arXiv:1010.5217.

[147] S.L. Glashow and S. Weinberg, *Phys. Rev.* **D15** (1977) 1958.

[148] G. Isidori, Y. Nir and G. Perez, *Annu. Rev. Nucl. Part. Sci.* **60** (2010) 355.